Check for updates

Energy & Environmental Materials WILEY

Silica Gel Supported Solid Amine Sorbents for CO_2 Capture

Baljeet Singh, Zahra Eshaghi Gorji, Rustam Singh, Vikas Sharma, and Timo Repo**

Point source CO_2 capture (PSCC) is crucial for decarbonizing various industrial sectors, while direct air capture (DAC) holds promise for removing CO_2 directly from the air. Sorbents play a critical role in both technologies, with their performances, efficiency, cost, etc., largely depending on which type is used (physical or chemical). Solid amine sorbents (SAS) employed in the chemical adsorption of CO_2 are suitable for both PSCC and DAC. SAS offer significant advantages over liquid amines such as monoethanolamine (MEA), due to their ability to perform cyclic adsorption–desorption with much lower energy requirement. The environmental concern associated with MEA can be mitigated by SAS. Support materials have a significantly important role in stabilizing amine and enhancing stability and kinetics; varieties of support materials have been screened at a laboratory scale. One promising support material is a silica gel (SG), which is commercially available and attractive for designing cost-effective sorbents for large-scale CO_2 capture. Various impregnation methods such as physical adsorption and covalent functionalization have been employed to functionalize silica surfaces with amines. This review provided a comprehensive critical analysis of SG-based SAS for CO_2 capture. We discussed and evaluated them in terms of their adsorption capacity, adsorption, and desorption conditions, and the kinetics involved in these processes. Finally, we proposed a few recommendations for further development of low-cost, lower carbon footprint SAS for large-scale deployment of CO_2 capture technology.

1. Introduction

Fossil fuels remain the primary source of energy for the most of world's electricity generation, making them one of the largest emitters of CO_2 in the energy sector.[1] In 1950, CO_2 emissions were approximately 6 billion tonnes, but today, over 37 billion tonnes of CO_2 are emitted annually, with the total greenhouse gas emissions surpassing 55 billion tonnes in 2021 (**Figure 1a,b**). As per the estimation, power generation from fossil fuels has increased by 70% since 2000. In the most populated countries, such as China and India, coal-based power generation accounts for more than 60% of their total CO_2 emission, underscoring the necessity of PSCC to mitigate further CO_2 accumulation into the atmosphere.[2]

Due to population growth and fast modernization, the energy demand is continuously increasing, suggesting that on average CO_2 emissions keep increasing over the next few decades. CO_2 emissions are the main driver of climate change, and reducing these emissions urgently is the only solution that remains. In the first quarter of 2023, European Union GHG emissions totaled 941 million tonnes of CO_2 equivalent. The primary contributors were household (24%), manufacturing (20%), electricity and gas supply (19%), agriculture (13%), followed by transportation and storage (10%).[3] The concentration of CO_2 in the atmosphere is increasing more rapidly than what is needed to limit the global warming level to 1.5 °C.[4–6] Therefore, innovation in CO_2 capture technology for decarbonizing various industries and utilizing captured CO_2 is essential for addressing these challenges.

The development of CO_2 capture technologies not only reduces CO_2 emissions but also creates a highly flexible system capable of leveraging a wide range of power generation options as per the economic situation.[7] Economically, poor countries may struggle to afford the high cost associated with developing renewable and green energy systems. However, they can integrate CO_2 capture technologies at their power plants to reduce emissions, providing valuable time for the transition from fossil-based to renewable-based, while combating rising global CO_2 levels. The designing and upscaling of low-cost CO_2 capture sorbents, along with ready-to-use or retrofitting systems, offers greater flexibility for low-income countries to diversify their power generation sources.[8] For large-scale CO_2 capture technology development, apart from machinery, sorbents are the key components due to the potential to drive technology advancement. Therefore, designing low-cost sorbents is crucial for cost reduction at the industrial level and enabling large-scale PSCC and DAC deployment. This involves creating more sustainable and efficient engineering solutions for large-scale CO_2 emission reductions.[9–11]

The scientific community is actively searching for potential sorbents for CO_2 capture (PSCC and DAC).[12–15] Various methods are under investigation, including liquid[16–19] and solid sorbents,[11,15,20–23] membrane-based separation,[24–28] and physisorption.[29–31] Energy consumption per ton of CO_2 capture varies depending on the process, type of sorbents used, and energy source involved. In addition to

Dr. B. Singh, Dr. Z. E. Gorji, Prof. Dr. T. Repo
Department of Chemistry, University of Helsinki, FI-00014, Helsinki, Finland
E-mail: baljeet.singh@helsinki.fi
E-mail: timo.repo@helsinki.fi
Dr. R. Singh
Jordi Labs, 200 Gilbert Street, Manfield, MA 02048, USA
V. Sharma
Centre for Converging Technologies, University of Rajasthan, Jaipur 302004, India
The ORCID identification number(s) for the author(s) of this article can be found under https://doi.org/10.1002/eem2.12832.

DOI: 10.1002/eem2.12832

© 2024 The Author(s). *Energy & Environmental Materials* published by John Wiley & Sons Australia, Ltd on behalf of Zhengzhou University. This is an open access article under the terms of the Creative Commons Attribution License, which permits use, distribution and reproduction in any medium, provided the original work is properly cited.

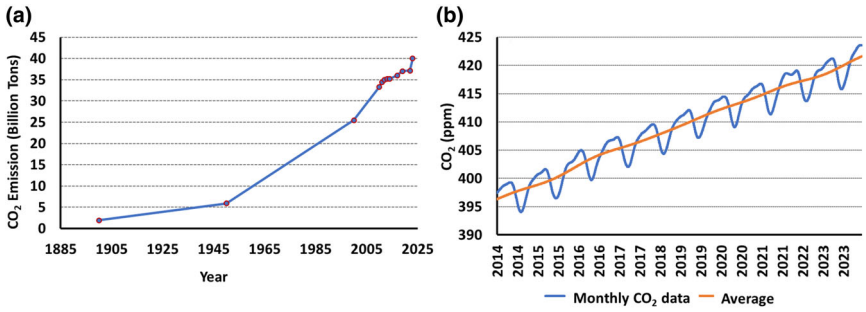

Figure 1. a) Annual CO_2 emission from fossil fuel and various industries globally. b) Recent global yearly mean CO_2 emissions data (data source: NOAA, measured at the Mauna Loa Observatory).[6]

designing cost-effective, efficient, and scalable sorbents, reducing the energy consumption per ton of CO_2 captured is also a major goal for big industries and startups. This can be achieved through diversification of energy sources, such as harvesting waste energy from industrial sources, recovering low-grade waste heat, or using renewable energy sources that could support regenerating sorbents with low carbon footprints.[32] The use of waste heat from different processes can reduce the overall cost of CO_2 capture and help in building a carbon-neutral/zero circular energy economy.[33] Possibly, the use of SAS allows exploration of different regeneration modes such as vacuum-temperature swing,[34] temperature swing,[35] or vacuum swing.[33,36] The sorbents must meet the following criteria to transition from lab-scale research to commercially viable products or technology:

- Low cost, simple to produce using green solvents, and scalable: Industries prefer processes or products that are low cost, simple and easy to produce, and scalable for profitability. Most of the lab-design sorbents are sophisticated entail multistage reactions and require the use of toxic solvents to synthesize support materials, making them difficult to scale up and expensive. Environmental concerns related to the use of toxic chemicals for porous support materials scaling up can be mitigated by designing water or green solvent-based simple synthesis procedures.
- High adsorption capacity: Sorbent should have a high adsorption capacity at low partial pressure (1–10 mmol g^{-1}), which will reduce the total amount of sorbent required for large-scale CO_2 capture.
- Low heat of regeneration: Sorbent should release adsorbed CO_2 at a low temperature. For example, SAS is generally heated up to 50–120 °C (depending on the use of vacuum along with direct heating), while physisorbed CO_2 can be recovered just by vacuum swing or mild heating (<50 °C). In the case of SAS, breaking a chemical bond between CO_2 and amine requires 2–3 GJ ton^{-1} of CO_2 compared to 4 GJ ton^{-1} of CO_2 in the case of MEA.[37]
- Fast adsorption kinetics: Sorbent should saturate quickly to allow for rapid adsorption–desorption cycles, accumulating more CO_2 than those with a long saturation time with high capture capacity. Amines are typically highly reactive to CO_2 and can reach 80–90% adsorption capacity within a few min, depending on the CO_2 concentration in a gas stream.[38,39]
- Fast desorption rate at low temperature: Sorbents with short adsorption–desorption cycles are preferred for industrial applications. Amine-based sorbents require moderate heating to regenerate sorbents as compared to MgO, and CaO-based systems.[40] Some modifications are reported to reduce the heat of desorption and to improve kinetics.[41] The changes in the regeneration methods, amine load, type of amines, support, and type of chemical species formed during adsorption can also affect the total regeneration energy requirement.[42–44]
- High selectivity for CO_2: Chemical adsorption is generally 100% selective to CO_2 compared to N_2 and O_2 unless other acidic gases are not present in the gas stream. Some MOFs are capable of physical adsorption of CO_2 with high selectivity;[45] however, the presence of NO_x/SO_x may degrade overall performance.[46]
- High-water tolerance: Air and flue gas typically contain a large amount of water; therefore, the sorbent's capacity and kinetics should not be negatively affected by the presence of water. In CO_2 capture process, water can be removed by condensation, and such a hybrid technology can produce water from the air and capture CO_2. SAS can perform better in the presence of a certain amount of water because amine efficiency (mmol of CO_2/mmol of amine) increases from 0.5 to 1 (**Scheme 1**).[47-49] However, water condensation inside the pores of support materials might impact the total adsorption capacity and add to the regeneration energy consumption.[50–53] In another scenario, excess water condensation could leach out physically adsorbed amines from support materials.
- High thermal and chemical stability: Since the flue gas temperature can vary in the range of 30–1200 °C, the sorbent should withstand a wide temperature range. SAS typically adsorbed maximum CO_2 at 75 °C; while lithium silicate-based sorbents can capture CO_2 even at a much higher temperature (>600 °C).[54] Amines are also well known for oxidative degradation under the influence of different CO_2 capture conditions.[55,56] However, in most cases, the energy and heat from high-temperature flue gases can be recovered by heat exchangers and a hybrid technology can be integrated to produce energy and capture CO_2.
- Large no. of adsorption–desorption cycles: Sorbents that can undergo many adsorption–desorption cycles are ideal for industrial applications. It will impact the total CO_2 adsorption in a lifetime and reduce the CO_2 capture cost.[57,58]

In this focused review, we discussed the synthesis of SAS using commercially available SG as support material. We summarized and covered the method of sorbent preparation and different parameters to tune adsorption capacity and desorption conditions. Challenges and suggestions for developing sustainable, low-carbon footprint SAS for selective CO_2 adsorption from various CO_2 sources are highlighted. A small section on silica aerogels-amine-based solid sorbents for CO_2 adsorption is also included.

2. Properties of Silica Gel

Silica has emerged as a promising support material for the large-scale production of SAS for industrial applications. Commercially available SG

© 2024 The Author(s). *Energy & Environmental Materials* published by John Wiley & Sons Australia, Ltd on behalf of Zhengzhou University.

25750356, 0, Downloaded from https://onlinelibrary.wiley.com/doi/10.1002/eem2.12832, Wiley Online Library on [10/12/2024]. See the Terms and Conditions (https://onlinelibrary.wiley.com/terms-and-conditions) on Wiley Online Library for rules of use; OA articles are governed by the applicable Creative Commons License

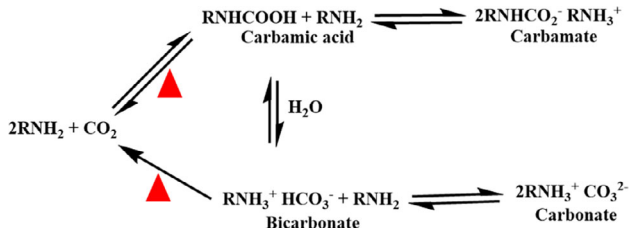

Scheme 1. General reactivity of CO_2 with amines.

Table 1. Textural properties and other details of commercially available SG and comparison with mesoporous silica.

Silica gel	Particle size (μm)	Surface area ($m^2 g^{-1}$)	Pore size (nm)	Pore volume ($cm^3 g^{-1}$)	Product no.	Cost per kg ($)
6–14 mesh	–	500	4	–	214 426-1kg	71.0
28–200 mesh	75–650	800	2.2	0.43	214 396-1kg	108.0
70–230 mesh	63–200	–	6	0.75	288 624-1kg	240.0
230–400 mesh	40–63	550	6	0.80	227 196-1kg	446.0
200–425 mesh	35–75	–	6	0.75	236 772-1kg	449.0
100–200 mesh	75–150	430–530	3	0.40	214 477-1kg	700.0
Mesoporous silica						
MCM-41[b]	100 nm	1000	2.1–2.7	0.98	643 653-5G	271.00
SBA-15[b]	<150 μm	700	6	0.5–0.7	914 614-5G	308.00
MSU-F (cellular foam)[b]	–	500–800[a]	2–50[a]	2.31	560 979-10G	239.40

[a]Value taken from literature, not provided by the supplier.
[b]Cost for large quantity (1 kg) is not available, unit prices are provided for comparison.

is a porous material with a moderate surface area, large pore volume, and wide pore size distribution (**Table 1**). It can be produced on a large scale with a price as low as $0.4 per kg; although, low-scale supply can be highly expensive, depending on the supplier, and forms of silica (Table 1). SG is used widely in industries and academia across different scales. Preparation or production of SG does not involve the use of any kind of deleterious solvents such as xylene, or cyclohexane, nor does it require surfactants like CTAB, P123, etc., which are commonly used for the preparation of mesoporous silica.[59–63] This makes SG a safer and more environmentally friendly option for developing SAS.

Mesoporous silica such as SBA-15, MCM-41, KCC-1, and MSU has better textural properties, including surface area, pore size distribution, and pore volume compared with commercially available SG. However, the synthesis of mesoporous silica involved the use of surfactant molecules such as CTAB and P123. Removing these surfactants typically requires heating at high temperatures (500–800 °C), which can increase the carbon footprints of the support materials themselves. Additionally, the overall waste (solid, liquid, and gases) generated from a synthesis of mesoporous silica support is substantial and often overlooked during the scaling up. The use of waste materials such as rice husk, blast furnace steel slag, fly ash, or low-cost silica precursors could reduce the cost of support production and could allow upscaling of low carbon footprints of support materials. In terms of cost, SG is significantly cheaper to produce than mesoporous silica (SBA-15, MCM-41, KCC-1, and MSU) (Table 1).

3. Silica Gel-based Solid Amine Sorbents

Silica has emerged as a potential support material for the large-scale production of SAS for industrial applications. For this, a variety of amines can be utilized to produce them for CO_2 capture applications. **Table 2** summarizes information about the commercially available amines, that have been explored for sorbents design at various levels.

Amines react readily with CO_2 at low partial pressure and can form various chemical species such as carbonate, bicarbonate, carbamate, and carbamic acid (Scheme 1). Theoretically, under dry conditions, 2 mol of amines can react with 1 mol of CO_2; however, reaction stoichiometry shifts to 1:1 in the presence of water. SAS are suitable for PSCC and DAC applications.[64,65]

The properties of support materials, such as surface area and pore size distribution, have a broad impact on amine loading, dispersion, CO_2 adsorption capacity, and kinetics. Since the production of silica support materials using traditional industrial methods is highly expensive and challenging, developing easy-to-produce sorbent materials is crucial for decarbonizing industries and achieving net zero CO_2 emissions by 2050. Silica-supported amines can drive large-scale advancement of CO_2 capture. The introduction of active functional groups ($-NH_2$) onto silica support is mainly achieved via four methods as described below:

i Physical impregnation or wet grafting (Class 1) (which includes post-synthesis modifications): In this method, as prepared silica is mixed with amine solution and dried using a vacuum under sufficient heating. Typically, these sorbents tend to be thermally less stable due to weak/poor physical interaction between support and amines. During cyclic adsorption–desorption, amines can vaporize, and overheating leads to thermal and oxidative degradation. However, the extent of degradation depends on several factors, such as the presence of impurities, desorption temperature, type of amine, and nature of support. Despite this, physical adsorption of amines on support materials is relatively easy to prepare and can achieve high amine loading with high capture capacity, offering the potential for quick upscaling to ton scale. This type of sorbent is referred to as Class 1 (**Figure 2**).

ii Covalent functionalization (Class 2): Covalently attached amines with silica surfaces are thermally more stable and have fewer chances to leach out during cyclic adsorption–desorption cycles. The availability of silanol (Si-OH) groups on the silica surface facilitates the formation of Si-O-Si bonds with different aminosilanes (Class 2 in Figure 2, Table 2, entry 15–19). However, this method requires special types of silanes, anhydrous conditions (dry toluene), and heating at high temperatures (80–120 °C). Loading of amines on silica is relatively limited due to the finite Si-OH groups on the silica surface. Each amino silane can utilize at least two to three Si-OH groups present on the silica surface (Class 2 in Figure 2). Some reports indicate that higher amine loading can be achieved through the in-situ generation of additional Si-OH groups (which are discussed in later sections).

© 2024 The Author(s). *Energy & Environmental Materials* published by John Wiley & Sons Australia, Ltd on behalf of Zhengzhou University.

25750356, 0, Downloaded from https://onlinelibrary.wiley.com/doi/10.1002/eem2.12832, Wiley Online Library on [10/12/2024]. See the Terms and Conditions (https://onlinelibrary.wiley.com/terms-and-conditions) on Wiley Online Library for rules of use; OA articles are governed by the applicable Creative Commons License

Table 2. Amines used for CO_2 adsorption and available commercially with product code, their properties with cost.

Sr. no.	Amine	Structure	Boiling point (°C)	Flash point (°C)	Product code	Cost per kg ($)
1	1,2-Bis(3-aminopropylamino)ethane (bisAPED)	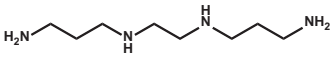	150	–	239399-100mL	40.40
2	2-Amino-2-methyl-1-propanol (AMP)	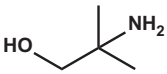	165	85	A65182-1L	67.00
3	Diethylenetriamine (DETA)	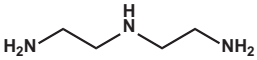	206	94	D93856-1L	81.50
4	Ethanolamine	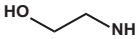	170	91	E9508-1L	86.70
5	Pentaethylenehexamine (PEHA)	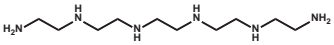	380	113	292753-1L	116.00
6	Tetraethylenepentamine (TEPA)	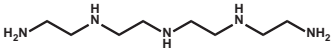	340	163	T11509-1Kg	118.00
7	1,4-Bis(3-aminopropyl)piperazine (bisAPPip)	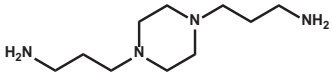	150	163	239488-50ML	130.00
8	Ethylenediamine	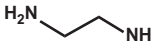	118	38	03550-1L	134.00
9	Hexamethylenediamine	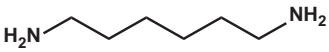	204	80	H11696-1KG	137.00
10	Polyethylenimine, linear	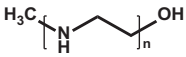	–	–	764604-1G	149.00
11	N,N′-Bis(2-hydroxyethyl)ethylenediamine	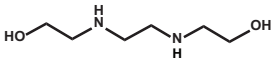	100 (mp)	–	268879-50G	247.00
12	Tris(2-aminoethyl)amine	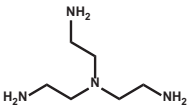	114	113	225630–100mL	266.00
13	Polyethylenimine, branched (PEI)	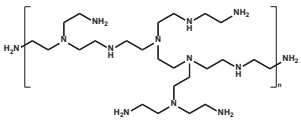	250	200	408727-1L	449.00

© 2024 The Author(s). *Energy & Environmental Materials* published by John Wiley & Sons Australia, Ltd on behalf of Zhengzhou University.

25750356, 0, Downloaded from https://onlinelibrary.wiley.com/doi/10.1002/eem2.12832, Wiley Online Library on [10/12/2024]. See the Terms and Conditions (https://onlinelibrary.wiley.com/terms-and-conditions) on Wiley Online Library for rules of use; OA articles are governed by the applicable Creative Commons License

Table 2. Continued

Sr. no.	Amine	Structure	Boiling point (°C)	Flash point (°C)	Product code	Cost per kg ($)
14	2-Amino-2-methyl-1,3-propanediol (AMPD)	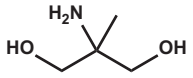	151	>100	A9754-500G	335.00
15	(3-aminopropyl) trimethoxysilane (AP-TMS)	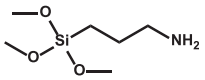	92	–	281778-500ML	266.00
16	[3-(2 Aminoethylamino)propyl] trimethoxysilane (AEAP-TMS)	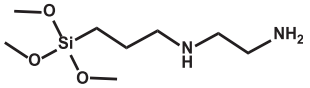	146	–	440302-500ML	176.00
17	N1-(3-Trimethoxysilylpropyl)diethylenetriamine (DETA-TMS)	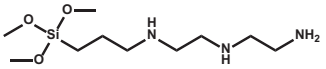	118	–	413348-500ML	255.00
18	Bis[3-(triethoxysilyl)propyl]amine (BTPA)	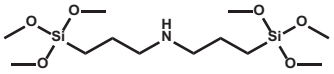	152	–	413356-50ML	73.90
19	(3-Aminopropyl) triethoxysilane (AP-TES)	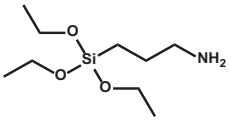	217	–	440140-500ML	345.00

iii In-situ polymerization (Class 3): The limitations of Class 1 and Class 2 can be addressed by increasing amine loading and directly covalent tethering of amine, which can be achieved by the in-situ polymerization of Class 2 amines or Class 1 polymers using another anchoring silane such as (3-glycidyloxypropyl)trimethoxysilane (GTMS). This method originally developed by Jonathan et al.[66] and classified as Class 3, involves the polymerization of amine monomers or in situ polymerization of silica precursor and amino silane (Figure 2).

iv Blending of amines (Class 4): While, Classes 1–3 were categorized and discussed by Christopher and team,[67] we have further ranked a newly emerging Class 4. This is referred to as the blend or a complex mixture of two to three different types of amines on a single or multiple support material.[68] The goal is to utilize the best properties of amines and synergistically stabilize sorbents against thermal and chemical degradation. In this class, amines are not necessarily covalently attached to the support materials (Figure 2).[69]

SG (with a surface area of 480 $m^2 g^{-1}$, pore volume of 0.81 $cm^3 g^{-1}$, and an average pore diameter of 6 nm) was surface modified by different molecular weight PEI (275, 800, 1800, and 25 000) through wet impregnation/physisorption method.[70] In this impregnation method, a stock solution of PEI in methanol was prepared, mixed with SG in different proportions, and stirred for 60 min. The solvent was then evaporated using a rotary evaporator at 70 °C, and the dried samples were used for CO_2 adsorption. The resulting SAS were analyzed based on different amine types, CO_2 adsorption kinetic, CO_2 capture capacity in the temperature range of 35–95 °C, sorbent regeneration, and cyclic adsorption–desorption performance (**Table 3**).

PEI(25000)/SG showed an improved CO_2 adsorption capacity with increasing temperature (35–90 °C), suggesting that the PEI(25000)/SG required a higher temperature to overcome the effect of PEI viscosity, reducing diffusion barriers and enhancing CO_2 adsorption. The impact of adsorption temperature could be different for different types of PEI. For example, PEI(800)/SG and PEI(1800)/SG achieved maximum adsorption capacity at 55 °C, while PEI(275)/SG showed the highest CO_2 adsorption capacity at 75 °C. This indicates that both viscosity and loading affect CO_2 adsorption performance at different adsorption temperatures. Overcrowding of amines can also reduce CO_2 adsorption capacity.

The CO_2 adsorption capacity of HMW PEI(25000)/SG was the lowest among all the samples (32 mg g^{-1} (0.72 mmol g^{-1}) at 75 °C and 48 mg g^{-1} (1.09 mmol g^{-1}) at 95 °C). LMW PEI(800)/SG exhibited CO_2 adsorption capacity of 91 mg g^{-1} (2.06 mmol g^{-1}) at 55 °C. Along with PEI, TEPA was also used for comparison, TEPA (37 wt.%)/SG sample showed a higher CO_2 adsorption capacity of 100 mg g^{-1} (2.27 mmol g^{-1}) at 75 °C.[70] The large CO_2 adsorption capacity of

© 2024 The Author(s). *Energy & Environmental Materials* published by John Wiley & Sons Australia, Ltd on behalf of Zhengzhou University.

25750356, 0, Downloaded from https://onlinelibrary.wiley.com/doi/10.1002/eem2.12832, Wiley Online Library on [10/12/2024]. See the Terms and Conditions (https://onlinelibrary.wiley.com/terms-and-conditions) on Wiley Online Library for rules of use; OA articles are governed by the applicable Creative Commons License

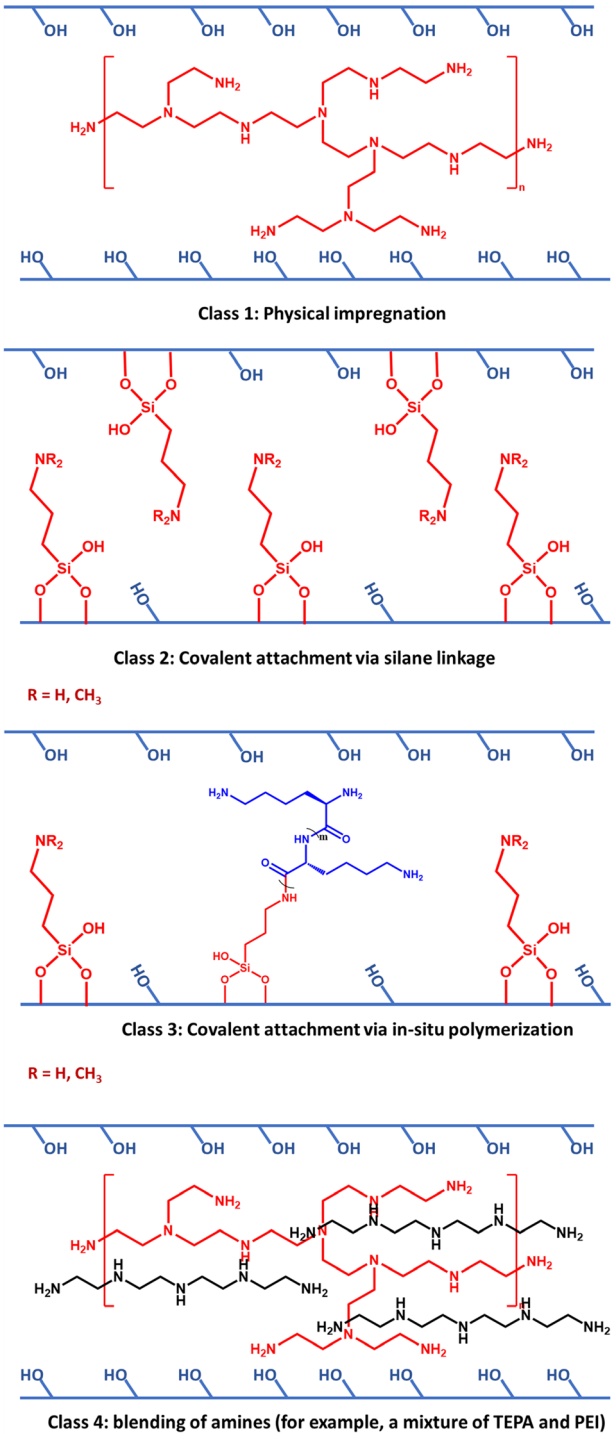

Figure 2. Four classes of silica-based SAS.

TEPA/SG could be due to the higher nitrogen content and small molecular size of TEPA compared to PEI. Moreover, PEI mostly has secondary amines which can reduce adsorption capacity compared to TEPA, which has two primary amines per molecule.[71–73]

Initially, CO_2 desorption/regeneration analysis was performed at 75 °C.[70] At this temperature, 58%, 80%, 85%, 84%, and 76% of maximum adsorption capacity was desorbed within 150 min for TEPA/SG, PEI(275)/SG, PEI(800)/SG, PEI(1800)/SG, and PEI(25000)/SG samples, respectively. The difference in desorption performance depends on the heat of adsorption, which is higher for primary amines and lower for secondary and tertiary amines. Thus, the TEPA/SG sample contains a large no. of primary amines which could require a higher temperature to desorb CO_2. As the desorption temperature was increased to 100 °C, all samples were fully regenerated within 120 min.

PEI(275)/SG, PEI(800)/SG, PEI(1800/SG), and TEPA/SG samples showed amine leaching and a decrease in CO_2 adsorption capacity during cyclic adsorption–desorption under identical conditions (**Figure 3**, Table 3), while HMW PEI(25000)/SG was found more suitable and exhibited complete regeneration at 100 °C. Also, it showed no change in adsorption capacity during 10 adsorption–desorption cycles (adsorption at 75 °C and desorption at 100 °C). TEPA/SG, PEI(275)/SG, PEI(800)/SG, and PEI(1800)/SG samples showed a decrease in adsorption capacity by 67%, 74%, 34%, and 35% within 10 cycles, respectively.

In another study, a series of PEI-functionalized sorbents were prepared through the wet-impregnation method.[74] The effect of pore size, PEI loading, and adsorption temperature in the range of 25–100 °C were investigated. Four variants of different PEI loading from 10 to 40 wt.% were analyzed. As the PEI loading increased from 10 to 30 wt.%, the CO_2 adsorption capacity rose from 18.8 to 93.4 mg g^{-1}. However, when PEI loading increased to 40 wt.%, CO_2 adsorption capacity decreased to 74.1 mg g^{-1}, which could be due to overloading and decrease of CO_2 diffusion in the pores. Pore size did not show any major impact from PEI loading, as it appeared to increase from 5.9 to 9 nm when PEI loading increased from 0 to 40 wt.%. However, N_2 sorption is typically measured at liquid nitrogen temperature (−77 K), which does not accurately represent the true pore size under CO_2 adsorption conditions. In addition, the overall sorbent cost was calculated to be around \$25/kg, which is significantly lower than \$760/kg for SBA-15, \$44/kg for low-grade porous carbon-based, and \$30/kg for Al_2O_3-based solid sorbents.[75–77] A cost of \$5/kg could lead to a very good scenario; therefore, the cost of \$10/kg could be a more economically viable option.[78]

The impact of particle size (33–75, 75–150, and 250–425 μm) and pore volume (0.68, 0.75, and 1.15 cm^3 g^{-1}) of SG was investigated.[79] Specific surface area, pore volume, and pore size distribution decreased as PEI loading increased to 60 wt.%. The surface area and pore size of PEI(50)/SG reduced from 260 to 35 m^2 g^{-1}, and 1.03 to 0.17 cm^3 g^{-1}, respectively. At 60 wt.% loading, neither pore volume nor surface area were measurable. Among different PEI loadings, the effects of adsorption temperature (**Figure 4a**), and moisture on the CO_2 adsorption capacity of PEI(50)/SG were studied in detail. The PEI/SG sample with 50 wt.% PEI loading showed an adsorption capacity of 138 mg g^{-1} (3.13 mmol g^{-1}) at 75 °C, which was found the same as for PEI/SBA-15 (Figure 4b, Table 3). At such a high loading pore size intensity was reduced to half of the original sample, which exhibited that only surface amines are important for adsorption. SBA-15 is one of the most versatile and highly explored silica supports for various applications including CO_2 capture.[80] As the molecular weight of PEI increases, CO_2 adsorption capacity is reduced likely due to the diffusion limitation, which was also investigated by Chen et al.[70] Elevated temperatures improved CO_2 adsorption by reducing PEI viscosity, enhancing molecular flexibility, and increasing accessibility.[62,81]

© 2024 The Author(s). *Energy & Environmental Materials* published by John Wiley & Sons Australia, Ltd on behalf of Zhengzhou University.

25750356, 0, Downloaded from https://onlinelibrary.wiley.com/doi/10.1002/eem2.12832, Wiley Online Library on [10/12/2024]. See the Terms and Conditions (https://onlinelibrary.wiley.com/terms-and-conditions) on Wiley Online Library for rules of use; OA articles are governed by the applicable Creative Commons License

Table 3. Type of SG used for sorbents design and their properties, information about the amine used, adsorption conditions, and corresponding CO_2 adsorption capacity.

Silica gel used	Textural properties SA ($m^2 g^{-1}$), PV ($cm^3 g^{-1}$), PS (nm)	Amine type	Amine loading (wt.%)	Adsorption capacity (mmol g^{-1})	Adsorption conditions	No. of cycle (capacity drop in total cycles)	References
Silica gel	480, 0.81, 2–10	PEI(275)	12.89	2	100% CO_2, 30 mL min^{-1}	10 (~74%)	[70]
		PEI(800)	12.65	1.79	Ads.: 75 °C	10 (~34%)	
		PEI(1800)	12.73	1.25	Des.: 100 °C	10 (~35%)	
		PEI(25000)	12.59	0.72		10 (neg.)	
		TEPA	14.62	2.27		10 (~67%)	
160–200 mesh	541, 0.80, 1–15	PEI(423)	30	2.12	15.1% CO_2 in N_2, 10 mL min^{-1}	5 (neg.)	[74]
					Ads.: 75 °C		
					Des.: 100 °C		
33–75 μm	260, 0.68, –	PEI(423)	50	1.37	15% CO_2, 4.5% O_2, in N_2		[79]
		PEI(25000)	40	1.76	20 mL min^{-1}		
		PEI(50000)	60	0.18	Des.: 100 °C for 240 min		
75–150 μm	–, 0.75, –	PEI(423)	60	1.72			
		PEI(25000)	50	0.272			
		PEI(50000)	40	0.25			
250–425 μm	–, 1.15, –	PEI(423)	40	0.12			
		PEI(25000)	60	0.17			
		PEI(50000)	50	0.17			
33–75 μm	260, 0.68, –	PEI(423)	50	2.97	100% CO_2, Ads.: 75 °C	10 (~4.6%)	
					Des.: 75 °C		
					100% CO_2, Ads.: 75 °C	10 (~11.6%)	
					Des.: 100 °C		

Values not provided; PS, pore size; PV, pore volume; SA, surface area.

Moisture levels in gas flow were also found to positively influence CO_2 adsorption capacity, with an optimum level of moisture consistently boosting the adsorption capacity.[79] 10 adsorption–desorption cycles were conducted using PEI(50)/SG as the best sample (33–75 μm, 50 wt.% loading, PEI 423 g mol^{-1}) (Figure 4c). While the adsorption was performed at 75 °C, the desorption was carried out at 75 and 100 °C (Table 3). A slight reduction in adsorption capacity with the number of cycles was observed with desorption at 100 °C. The CO_2 adsorption capacity reduced from 131 to 116 mg g^{-1} within 10 cycles, which accounts for approximately 11.6% reduction in adsorption capacity. Desorption at 75 °C maintained CO_2 adsorption capacity at around 95% of the original (Figure 4c). Desorption is always preferred at lower temperatures to decrease the total energy cost per ton of CO_2 captured.

TGA and a fixed bed reactor were used to compare the two sorbents under identical conditions (Figure 4d). Based on TGA results, the mass-based CO_2 adsorption capacity of PEI(50)/SG (131 mg g^{-1}) matched to the PEI(50)/SBA-15 (136 mg g^{-1}). Additionally, the adsorption capacity of PEI(50)/SG (138 mg g^{-1}) and PEI(50)/SBA-15 (140 mg g^{-1}) was almost the same in the fixed bed reactor. Notably, the volume-based adsorption capacity of PEI(50)/SG surpassed PEI (50)/SBA-15 in the fixed bed reactor, which was 83 and 32 mg g^{-1}, respectively (Figure 4d). The higher volume capacity of PEI(50)/SG could be due to higher packing density (0.60 g cm^{-3}) than that (0.23 g cm^{-3}) of PEI(50)/SBA-15. The calculated cost of support materials such as MCM-41, and SBA-15 were extremely high ($700/kg), way more than the amine itself.[79] Hence, designing a cost-effective SAS with a lower carbon footprint and cost present a significant challenge for industries.

There is a high demand for an economically viable and straightforward method to produce low-cost industrial-grade SAS. In another study, SG was surface-modified with DETA by impregnation method (Class 1, Figure 2).[82] Increasing DETA loading from 10% to 80% reduced the specific surface area of SG from 604 to 27 $m^2 g^{-1}$. Notably, higher amine loading does not necessarily translate to high adsorption capacity, as long as a few layers of amine can be accessible to CO_2 under given conditions. The utilization of the available surface area of support materials to achieve maximum CO_2 adsorption capacity is consistently preferred. However, pore size after amine impregnation determines the accessibility and CO_2 adsorption capacity which were consistently decreased with increasing DETA loading.

Fast adsorption–desorption cycles are essential for optimal industrial-grade SAS. DETA functionalized SG (FS-DETA) exhibited two distinct adsorption stages.[82] Upon exposure to 100% CO_2 (60 mL min^{-1}), a rapid weight gain was observed, achieving around 70% adsorption capacity achieved within 1 min, followed by slow adsorption over the remaining 249 min (reaching a maximum adsorption capacity of 40 mg g^{-1} for 10% DETA loading). The fast kinetics

© 2024 The Author(s). *Energy & Environmental Materials* published by John Wiley & Sons Australia, Ltd on behalf of Zhengzhou University.

25750356, 0, Downloaded from https://onlinelibrary.wiley.com/doi/10.1002/eem2.12832, Wiley Online Library on [10/12/2024]. See the Terms and Conditions (https://onlinelibrary.wiley.com/terms-and-conditions) on Wiley Online Library for rules of use; OA articles are governed by the applicable Creative Commons License

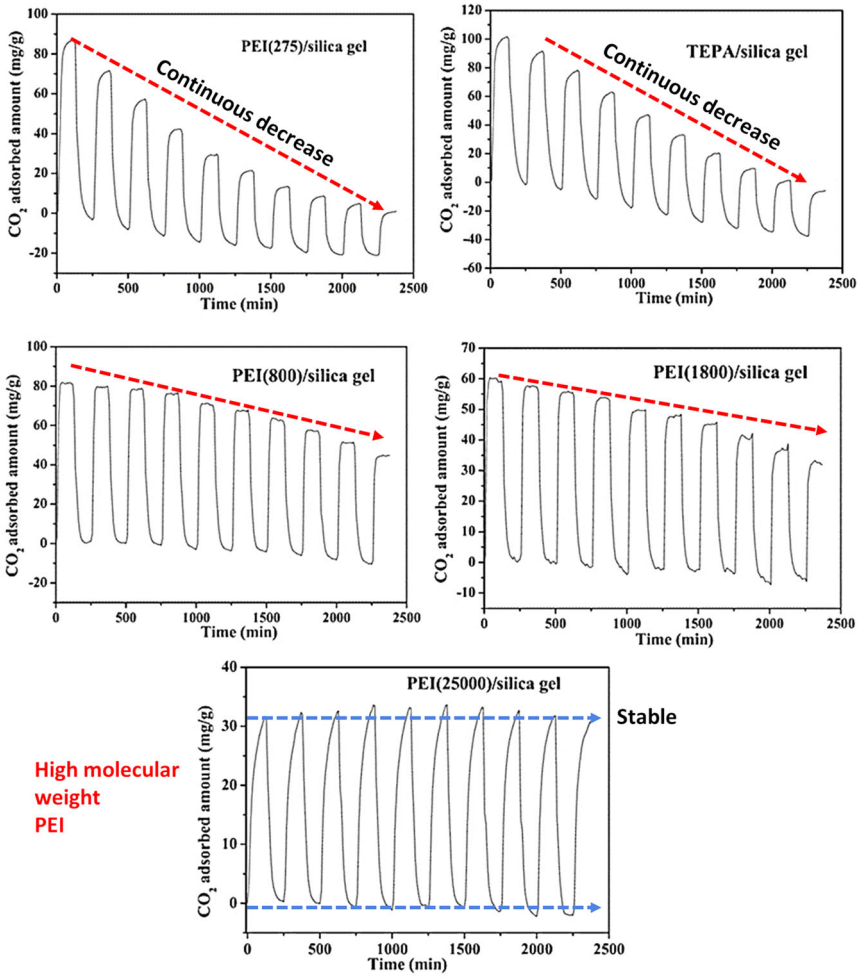

Figure 3. Cyclic adsorption–desorption of sorbents (adsorption at 75 °C and desorption at 100 °C, examined by TGA). The figure is reproduced with permission, Copyright-2017, John Wiley and Sons.[70]

can be attributed to the highly exposed surface layers of amine and enhanced pore accessibility. Subsequently, the second stage entails the gradual diffusion of CO_2 molecules within the less accessible pores. Higher amine loading can lead to overcrowding of the surface, reduce pores size, and hinder CO_2 diffusion to the active amine adsorption sites. It was observed that pore size decreased considerably when DETA loading increased from 10% to 80%. Therefore, optimal amine loading is imperative to maximize surface utilization and reduce pore blockage and CO_2 adsorption capacity. Cyclic adsorption–desorption was also performed for FS-DETA-10% and FS-DETA-40% (**Table 4**). The sorbent materials showed reproducibility of CO_2 adsorption capacity; however, a gradual decrease in adsorption capacity was detected, which could be due to incomplete desorption of CO_2, and evaporation of DETA.[82]

The low thermal stability of amines poses a significant operational challenge, and additionally, physisorbed amines slowly vaporize during adsorption–desorption cycles.[83] As mentioned earlier, two methods were used to produce SAS, that is, covalent attachment and physisorption. For covalent functionalization, AP-TMS, AEAP-TMS, and DETA-TMS were utilized. For this, SG was suspended in toluene with a desired amine and refluxed for 7 h, the resulting samples were dried and used as prepared. For physisorption, a branched polyethyleneimine (PEI, M_n – 600 g mol^{-1}, M_w – 800 g mol^{-1}), TEPA, bisAPED, and bisAPPip were employed for the CO_2 adsorption study. Furthermore, the primary amines of TEPA were also modified to secondary amines, which were named TEPAAN1 (TEPA:AN = 3:2) and TEPAN2 (TEPA:AN = 1:2), by a reaction between R-NH_2 and CH_2 = CH-CN to R-NH-CH_2-CH_2-CN (amination of acrylonitriles).

For the impregnation, the required quantity of amine was diluted in ethanol and mixed with SG. The final composite mixture of SG and amine was dried in an oven at 50 °C for 4–5 h. The specific surface area, pore volume, and pore size distribution were changed with loading, due to empty spaces of pore being occupied by amines. The CO_2 adsorption capacity of the samples was in the order of AEAP-TMS (~0.8 mmol g^{-1}, at 2.8 mmol g N^{-1}, 30% CO_2, 50 °C) > DETA-TMS (~0.6 mmol g^{-1}, at 3.3 mmol g N^{-1}, 30% CO_2, 323 K) > AP-TMS (~0.4 mmol g^{-1}, at 1.5 mmol g N^{-1}, 30% CO_2, 50 °C) (Table 4). Diamine (AEAP-TMS) exhibited the highest adsorption capacity. The adsorption efficiency of AP-TMS and AEAP-TMS, representing the ratio of adsorbed CO_2 per number of amine groups, ranged from 0.2 to 0.3. Additionally, DETA-TMS showed approximately 30% lower adsorption capacity, suggesting that only two out of three amines were accessible to CO_2 adsorption. To further examine the role of primary, secondary, and tertiary amines in CO_2 adsorption, two cases were considered. BisAPPip (containing two primary amines, and two tertiary amine groups) adsorbed less CO_2 than bisAPED (containing two primary and two secondary amine groups). The amine efficiency of bisAPPip was 0.25, indicating minimal contribution from tertiary amines to CO_2 adsorption. Branched PEI, containing a mixture of primary, secondary, and tertiary amines, exhibited CO_2 adsorption capacity in between bisAPED and bisAPPip (Table 4).

The physisorption of amine on a silica surface is not constrained by the availability of the Si-OH group on the silica surface. For physisorbed samples, the adsorption temperature was increased to 75 °C to avoid mass transfer limitations. TEPA and bisAPED showed almost similar CO_2 adsorption capacity in the range of 1.8–2 mmol g^{-1}, while PEI/SG showed a CO_2 adsorption capacity of around 1.6 mmol g^{-1}. However, acrylonitrile-modified TEPA showed a significant degradation in adsorption capacity. In the case of the TEPA-AN1 sample, the primary amine was partially converted to the secondary amine, resulting in a moderate adsorption capacity of 1.6 mmol g^{-1}, similar to PEI/SG. Diffusion of CO_2 molecules in solid sorbents is highly important and depends on the gas velocities, amine loading, and accessibility of active sites. The diffusion coefficient of CO_2 was determined by simulating breakthrough curves and was found to range from 2 to 5 × 10^{-11} m^2 s^{-1}.

Covalent attachment (grafting) of amine onto the silica surface can yield more stable and leach-proof SAS capable of withstanding direct

© 2024 The Author(s). *Energy & Environmental Materials* published by John Wiley & Sons Australia, Ltd on behalf of Zhengzhou University.

25750356, 0, Downloaded from https://onlinelibrary.wiley.com/doi/10.1002/eem2.12832, Wiley Online Library on [10/12/2024]. See the Terms and Conditions (https://onlinelibrary.wiley.com/terms-and-conditions) on Wiley Online Library for rules of use; OA articles are governed by the applicable Creative Commons License

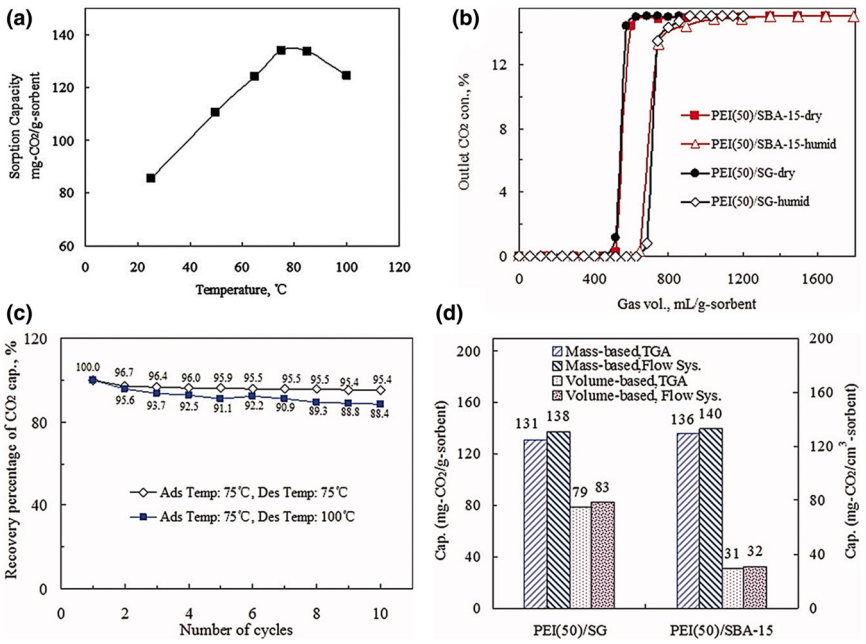

Figure 4. a) Effect of adsorption temperature. b) breakthrough curves of PEI(50)/SBA-15 and PEI(50)/SG for CO_2 adsorption from the stimulated flue gas (15% CO_2, 4.5 v% O_2 in N_2) in the presence/absence of moisture at 75 °C for 207 h^{-1} GHSV in the fixed-bed flow adsorption system. c) Recovery percentage of CO_2 capacity as a function of adsorption–desorption cycles. d) The CO_2 mass-based and volume-based adsorption capacity of PEI(50)/SBA-15 and PEI(50)/SG measured in TGA with pure CO_2 gas and the fixed-bed flow system with the simulated gas (15% CO_2, 4.5 v% O_2 in N_2) both at 75 °C. The figure is reproduced with permission, Copyright-2011, John Wiley and Sons.[79]

contact with steam. However, amine loading is on average, one silane can consume 2–3 silanol groups (Si-OH); hence, loading is limited by -OH availability. To improve amine loading, water is introduced during the grafting process to hydrate the silane (Si-O-Si) group, thereby increasing OH group density.[60] This process significantly improved amine loading on silica, known as the wet-impregnation method. A series of SG were covalently functionalized using DETA-TMS with a small amount of water, instead of using complete anhydrous conditions.[84] Initially, three SG with pore sizes of 22 Å, 66 Å, and 150 Å were grafted using triamine (DETA-TMS) and subsequently compared for CO_2 adsorption analysis, final samples were named AG-150A, AG-60A, and Ag-22A. AG-150A, AG-60A, and AG-22A exhibited CO_2 adsorption capacity of 1.35 mmol g^{-1} (amine loading of 3.39 mmol g^{-1}), 1.46 mmol g^{-1} (amine loading of 4.13 mmol g^{-1}), and 0.66 mmol g^{-1} (amine loading of 2.45 mmol g^{-1}), respectively (**Figure 5**a, Table 4). Despite low amine loading in the case of AG-150A sample, the CO_2 adsorption capacity was not significantly lower than AG-60A sample. AG-150A silica with higher amine loading (5.12 mmol g^{-1}) was further utilized for the wet grafting process. The results showed that the CO_2 adsorption capacity improved to 1.97 mmol g^{-1} at 25 °C and 1 bar pressure. The 0.15 mL of water was found sufficient to increase the optimal amine loading and maximize the CO_2 adsorption capacity (2.3 mmol g^{-1} at 75 °C, 1 bar).

The adsorption rate of CO_2 was measured for W-AG-150A at two different temperatures 25 and 75 °C, using 70% CO_2 in helium. The CO_2 adsorption capacity after 200 min was 65.9 mg g^{-1} (1.49 mmol g^{-1}) and 75.2 mg g^{-1} (1.70 mmol g^{-1}) at 25 and 75 °C, respectively (Figure 5b, Table 4). W-AG-150A sample was also evaluated for CO_2 adsorption under flue gas conditions (1.83 mmol g^{-1} at 75 °C, 0.15 bar). The stability of W-AG-150A was investigated via multiple adsorption–desorption cycles at 75 °C and desorption at 90 °C (Figure 5c). After 17 cycles, W-AG-150A showed no degradation in adsorption capacity. Additionally, fixed bed breakthrough curves were constructed under 415 ppm of CO_2 feed, at 25 °C. The adsorption capacity was 0.773 and 1.098 mmol g^{-1} under dry and wet conditions, respectively (Figure 5d). In the presence of water, large amounts of carbonate ion pairs were formed, which could enhance the amine efficiency.

The impact of the double functionalization method on CO_2 adsorption performance by blending covalently attached amine with PEI or TEPA was also investigated.[85] For SAS preparation, the desired amount of PEI or TEPA solution in methanol was mixed by sonication, and a certain amount of AP-TMS pre-functionalized SG was added. After 30 min, the mixture was dried at 60 °C for 12 h and used for CO_2 adsorption study. Different trends were observed for double-functionalized 1 N/SG (AP-TMS/SG). The maximum efficiency was 0.46 at 0 wt.% loading, which is close to the theoretical amine efficiency of 0.5 under dry conditions. With 30.4 and 26 wt.% loading of TEPA and PEI on 1 N/SG, the amine efficiency improved to 0.304 and 0.286, respectively, which was lower than the 1 N/SG sample. Because higher loading reduces CO_2 diffusion, all amine sites are not accessible to CO2. However, the amine efficiency of 3 N/SG (DETA/TMS/SG) was comparable to impregnated amine (Table 4). The maximum adsorption capacities of 10.4% and 9.7% were obtained for 3 N/SG/TEPA (19.1 wt.% loading) and 3 N/SG/PEI (10.6 wt.% loading), respectively.

Indeed, covalent functionalization of amine on silica surfaces results in better thermal stability during adsorption–desorption cycles; however, they have limited adsorption capacities due to a low amount of N content per unit weight of sorbent. Increasing the amine loading was explored by using varieties of silane containing more than one N such as AEAP-TMS, and DETA-TMS.[86] Under wet grafting of triamine (using a mixture of toluene and water) at the optimum temperature of 95 °C, achieved a CO_2 adsorption capacity of 2.61 mmol g^{-1}. Sorbent showed excellent cyclic stability for more than 100 cycles with a working capacity of 2.30 mmol g^{-1} (**Figure 6**a). On the contrary, TEPA-impregnated sorbent performance decreases with each cycle, which could be due to TEPA leaching from silica surface during a cyclic adsorption–desorption (Figure 6b).

4. Silica-Aerogel Supported Solid Amine Sorbents

Jiang et al.[87] developed a novel and low-cost spherical amine grafted silica aerogel (SASAs) for CO_2 capture. The spherical SG was prepared by dropping a sodium silicate-based silica sol and water mixture into a hot oil. After amine grafting by AP-TMS, the spherical SG was dried under a vacuum to prepare SASAs. Amine loading on spherical silica

© 2024 The Author(s). *Energy & Environmental Materials* published by John Wiley & Sons Australia, Ltd on behalf of Zhengzhou University.

25750356, 0, Downloaded from https://onlinelibrary.wiley.com/doi/10.1002/eem2.12832, Wiley Online Library on [10/12/2024]. See the Terms and Conditions (https://onlinelibrary.wiley.com/terms-and-conditions) on Wiley Online Library for rules of use; OA articles are governed by the applicable Creative Commons License

Table 4. Type of SG used for sorbents design and their properties, information about the amines used, adsorption conditions, and corresponding CO_2 adsorption capacity.

Silica gel used	Textural properties SA ($m^2 g^{-1}$), PV ($cm^3 g^{-1}$), PS (nm)	Amine type	Amine loading (wt.%)	Adsorption capacity (mmol g^{-1}) (adsorption temp. °C)	Adsorption conditions	No. of Cycle (capacity drop in total cycles)	References
0.2–0.5 mm	603.8, 0.52, 0.5–4 nm	DETA	10	0.91 (25 °C)	100% CO_2	4 (~0.36%)	[82]
				0.88 (30 °C)	60 mL min^{-1} for 250 min		
				0.44 (75 °C)			
			40	0.69 (25 °C)		4 (~4.87%)	
				0.68 (30 °C)			
				0.44 (75 °C)			
Grace X254	552, 0.84, 3–8 nm	AP-TMS	1.5[a]	0.4 (50 °C)	15% CO_2	–	[83]
		AEAP-TMS	2.8[a]	0.8 (50 °C)	Des.: 120 °C	–	
		DETA-TMS	3.3[a]	0.6 (50 °C)		–	
		bisAPED	7.8[a]	2.62 (50 °C)		5 (~60%)	
		bisAPPip	7.1[a]	1.52 (50 °C)		–	
		PEI	7.7[a]	1.49 (50 °C)		5 (~50%)	
		TEPA	–	2.0 (75 °C)		5 (~50%)	
		TEPAN1	–	1.6 (75 °C)		5 (~25%)	
		TEPAN2	–	0.61 (75 °C)		5 (~16%)	
22A (28–200 mesh)	805, 0.43, 2.2	DETA-TMS	2.45[a]	0.66	70% CO_2. 1 bar, 25 °C	-	[84]
60A (70–230 mesh)	338, 0.84, 6.0		4.13[a]	1.46		-	
150A	309, 1.12, 14.9		3.39[a]	1.35		-	
(200–425 mesh)		Wet impregnated	5.12[a]	1.97 (2.3 at 75 °C)		17 (neg.)	
(Davisil 646) (35–60 mesh)		SG	0	0.13	100% CO_2, 100 mL min^{-1} Ads.: 75 °C for 30 min		[85]
		AP-TMS	1.4[a]	0.63			
		DETA-TMS	4.23[a]	1.36			
		TEPA	41.7 (9.7[a])	3.31			
		PEI (1800)	37.7 (9[a])	2.63			
		AP, TEPA	30.4 (8.68[a])	2.63			
		AP, PEI	26% (7.62[a])	2.18			
		DETA-TEPA	19.1% (8.92[a])	2.36			
		DETA-PEI	10.6% (6.66[a])	2.20			

[a]Nitrogen contents (mmol g^{-1}) #in the presence of moisture, SA-surface area, PV-pore volume, PS-pore size.

aerogel increased with reaction time, which led to a sharp decrease in surface area and pore volume (**Table 5**). SASAs exhibited pore size distribution in the range of 3–20 nm, where large pores (>10 nm) were gradually blocked as amine loading increased, shifting the distribution to the 3–10 nm range. Excessive amine loading decreased CO_2 adsorption capacity, likely due to reduced pore size and accessibility of active amine sites. The maximum CO_2 adsorption capacity was 1.56 mmol g^{-1} with dry 1% CO_2 at 35 °C for SASA-3.

In another work, sodium silicate sol prepared from water glass was used for the preparation of porous SG beads.[88] These SG beads were impregnated by AP-TMS and PEI, and the effect of amine loading was evaluated for CO_2 adsorption at different temperatures. The 15 and 5 wt.% PEI loadings on these SG beads exhibited maximum adsorption capacity of 1.16 and 0.88 mmol g^{-1} at 50 °C, respectively. SiO_2-2% AP-TMS sample showed CO_2 adsorption capacity of 0.67 mmol g^{-1}, which is around 23.8% lower than the 5 wt.% PEI loading. Whereas TEPA and PEI-impregnated silica aerogel (SA) showed a CO_2 adsorption capacity of 6.1 mmol g^{-1} at 75 °C, and 3.3 mmol g^{-1} at 25 °C using 100% CO_2, respectively.[89,90] Furthermore, amine-functionalized SA also exhibited CO_2 adsorption capacity of 1.07 mmol g^{-1} under very diluted CO_2 (2500 ppm) at 22 °C.[91–93]

Recently, Yang and coworkers explored organic–inorganic hybrid aerogels (OIHAs) prepared from bis[3-(triethoxysilyl)]amine (BTPA) and methyltrimethoxysilane (MTES).[94] The presence of the CH_3 group makes the preparation process simpler and faster. The amine group from BTPA self-catalyzed the hydrolysis and condensation reaction between two silicon precursors to build a uniform mesoporous and macroporous structure. The high specific surface area and presence of the -NH groups resulted in the high CO_2 capture capacity of 5.89 mmol g^{-1} at 25 °C and 100 kPa. Interestingly, aerogel maintained

© 2024 The Author(s). Energy & Environmental Materials published by John Wiley & Sons Australia, Ltd on behalf of Zhengzhou University.

25750356, 0, Downloaded from https://onlinelibrary.wiley.com/doi/10.1002/eem2.12832, Wiley Online Library on [10/12/2024]. See the Terms and Conditions (https://onlinelibrary.wiley.com/terms-and-conditions) on Wiley Online Library for rules of use; OA articles are governed by the applicable Creative Commons License

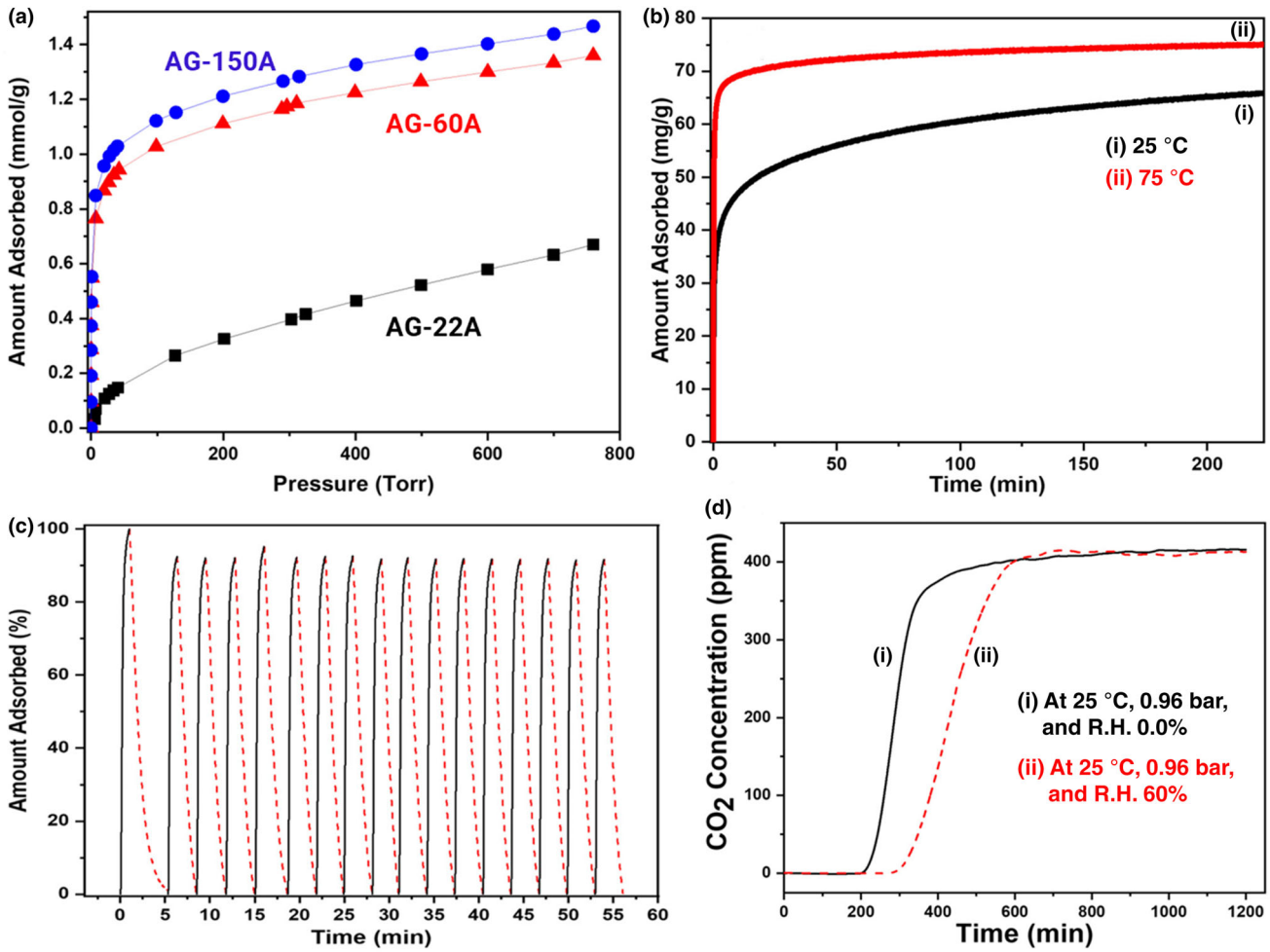

Figure 5. a) CO_2 adsorption isotherms of AG-22A (black), AG-60A (red), and AG-150A (blue), at 25 °C. b) CO_2 uptake rate on wet-grafted W-AG-150A at 25 °C (a) and 75 °C (b) under the 70% CO_2 in helium. c) Cyclic stability studies (70% CO_2 (in helium) flow, desorption in helium at 90 °C (dashed line) of wet-grafted W-AG-150A at 75 °C, and 1 bar. d) CO_2 breakthrough curve for wet-grafted W-AG-150A under the ambient air feed at 25 °C, space velocity 6500 h^{-1}. The figure is reproduced with permission, Copyright-2019, American Chemical Society.[84]

the adsorption capacity of 5.45 mmol g^{-1} after six cycles, retaining more than 92% of the initial adsorption capacity. The development of SAS by simple, cost-effective, and environmentally friendly methods is important for the large-scale deployment of CO_2 capture technology. Amine hybrid silsesquioxane aerogel (AHSA) was prepared using a single-step sol–gel process, and aerogel was dried using a supercritical CO_2 method, which helps retain porous structure.[95] For the preparation, 3-(aminopropyl)triethoxysilane was mixed with TEOS in a solvent mixture of ethanol and water. Finally, after 10 min, aerogel was washed with ethanol and dried by supercritical CO_2. When AHSA was exposed to 1% CO_2 at 50 °C, AHSA exhibited a CO_2 adsorption capacity of 3.84 mmol g^{-1} (humid). This method of preparation of SAS is indeed simple and effective for large-scale production. Hybrid one-pot aerogel outperformed mesoporous silica-based SAS at given conditions.

A new hybrid titania/silsesquioxane composite aerogel (AHTSA) was prepared using a one-pot method followed by supercritical drying.[96] The pore size distribution did not show any major impact of increasing amine loading; however, the intensity of smaller pores decreased, while large pores (100 nm) increased in the network. Specific surface area and mesoporous pore volume decreased with increasing amine loading. Generally, optimized amine loading played an important role in maximizing CO_2 adsorption. The effect of amine loading on CO_2 adsorption performance was investigated. As shown in Figure 6c, AT-10 had the maximum adsorption capacity of 4.19 mmol g^{-1}. Initially, CO_2 adsorption capacity enhanced with increasing amine loading and then decreased at higher amine loading. This could be due to the accessibility of surface-adsorbed CO_2 rather than the total amine load in the matrix. Regardless of amine loading, high surface area and pore volume, along with a wide pore size distribution, ultimately determine the accessibility of adsorption sites. CO_2 adsorption capacity of AHTSA increased from 1.64, 4.19, to 6.66 mmol g^{-1} when CO_2 concentration of a gas mixture changed from 400 ppm to 1% to 10%, at 30 °C with a gas flow of 300 mL min^{-1}, respectively (Figure 6c). High adsorption CO_2 favors the diffusion in the pores, and the interaction between surface amines and CO_2. Amine aerogel showed a short halftime and high amine efficiency across different CO_2 concentrations, indicating that the AHTSA is an effective and dynamic sorbent for DAC. AT-10 (8.47 mmol g^{-1}

© 2024 The Author(s). *Energy & Environmental Materials* published by John Wiley & Sons Australia, Ltd on behalf of Zhengzhou University.

25750356, 0, Downloaded from https://onlinelibrary.wiley.com/doi/10.1002/eem2.12832, Wiley Online Library on [10/12/2024]. See the Terms and Conditions (https://onlinelibrary.wiley.com/terms-and-conditions) on Wiley Online Library for rules of use; OA articles are governed by the applicable Creative Commons License

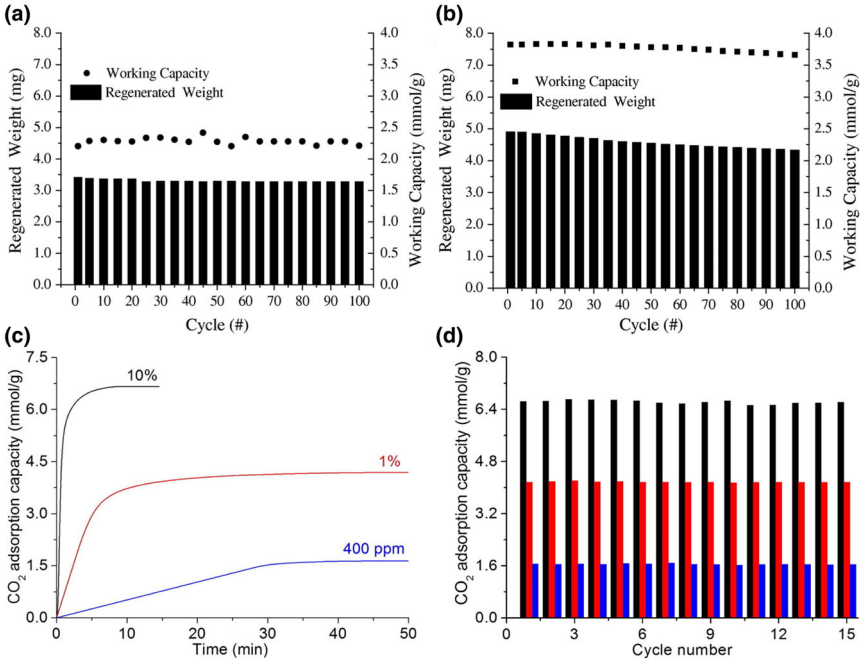

Figure 6. Cyclic working capacity and absolute regeneration weight of a) triamine grafted SA and b) 70 wt.% grafted SA. The figure is reproduced with permission, Copyright-2014, Elsevier.[86] c) CO_2 adsorption profile and capacities of AT-10 with different CO_2 concentrations. d) Cyclic CO_2 adsorption–desorption of AT-10 in dry air (blue/lowest), 1% (red/middle), and 10% (Black, highest). The figure is reproduced with permission, Copyright-2016, Elsevier.[96]

amine load) showed no degradation in adsorption capacity after 15 adsorption–desorption cycles (Figure 6d). A maximum amine efficiency of 0.79 was achieved with AT-10, along with excellent stability and reproducibility after 15 cycles, making amine-containing hybrid aerogels a promising sorbent for large-scale applications.

Amine hybrid zirconia/silica composite aerogel (AHZSA) was also investigated as a potential low-cost, simple to upscale, and environmentally friendly solid sorbent for CO_2 capture applications.[97] The CO_2 adsorption capacity of AHZSA was 2.70, 2.10, 2.00, and 1.48 mmol g^{-1} at 20, 50, 70, and 90 °C respectively. The hybrid aerogel CO_2 adsorption capacity increased to 3.40 mmol g^{-1} with the introduction of moisture in CO_2 flow (Table 5). In another study, amine hybrid resorcinol-formaldehyde/silica composite aerogel was developed, exhibiting CO_2 adsorption capacity of around 1.80, and 2.57 mmol g^{-1} under dry and humid conditions, respectively, at 25 °C.[98]

In the case of physisorbed amine on SG, amine degradation and slow vaporization during cyclic adsorption–desorption pose significant challenges, whereas covalently attached amines are more stable and leach-proof. These materials easily surpass other aerogel-type sorbents such as amine hybrid resorcinol-formaldehyde/silica composite aerogel,[99] chitosan aerogel,[100] CO_2 aerogel,[101] and PEI functionalized mesoporous silica (2.36 mmol g^{-1} at 25 °C, adsorption from the air).[102] Linneen et al.[103] used an impregnated method to immobilize TEPA on both hydrophobic (SA-O) and hydrophilic (SA-I). As prepared samples showed a pore size of 42 nm for SA-I and 21 nm for SA-O, which reduced from 42 to 5 nm as TEPA loading increased to 80%. However, higher amine loading does not necessarily result in higher adsorption capacity. As TEPA loading increased, CO_2 adsorption capacity enhanced from 2.2 to 6 mmol g^{-1} for SA-I-80 at 100% CO_2. However, by decreasing the CO_2 concentration to 10% in Ar, the CO_2 adsorption capacity was reduced to 3.5 mmol g^{-1} with an amine efficiency of 0.17%. To demonstrate the industrial applications, SA-I-80 was checked for 10 adsorption–desorption cycles using 100% CO_2.

As expected, hydrophilic aerogel-TEPA (SA-I-x) sorbents outperformed hydrophobic sorbents (SA-O-x), because water improves the adsorption performance (Table 5). 80 wt.% TEPA loading on SA-I showed CO_2 adsorption capacity of 3.5 and 6.1 mmol g^{-1} when exposed to 10% and 100% CO_2, respectively. Cyclic adsorption–desorption was performed, and the sorbent was able to maintain 5.1 mmol g^{-1} adsorption capacity over 10 cycles at 75 °C. The hydrophilic character of silica aerogel not only improves the adsorption capacity and amine efficiency but also reduces the time required to reach 90% equilibrium adsorption capacity. A better distribution of TEPA on SA-I increases adsorption kinetics.

In another work, Kong et al.[104] developed a one-pot sol–gel process using solvent exchange and supercritical CO_2 drying (SCD) to synthesize SAS. The effect of acetone, methanol, and ethanol solvents for solvent exchange on CO_2 adsorption capacity was also performed. A-SCD-acetone exhibited the highest CO_2 adsorption capacity of 5.55 mmol g^{-1} followed by A-SCD-ethanol (4.3 mmol g^{-1}) and A-SCD-methanol (3.9 mmol g^{-1}), due to aerogel's better surface area, pore size, and pore volume (**Figure 7a**). A-SCD-acetone showed adsorption capacities of 5.55, 5.0, and 3.97 mmol g^{-1} at 25, 50, and 75 °C, respectively. The A-SCD-acetone was investigated for 50 adsorption–desorption cycles at 25 °C with excellent stability and recyclability as there was no evident decrease in adsorption capacity in 50 cycles (5.55–5.50 mmol g^{-1}) (Figure 7b). The chemically fixed amines are much more robust, and stable compared to physically adsorbed amines. Kong et al.[105] also compared supercritical drying and ambient pressure drying methods to prepared SAS. Sorbent prepared by supercritical drying outperformed the ambient pressure dried sample, with a maximum CO_2 adsorption capacity of 4.51 mmol g^{-1} for 1% CO_2.

Hybrid aerogels, such as cellulose/silica, have the potential to enhance physical adsorption of CO_2.[106] The CO_2 uptake of composite aerogel was measured using thermal swing cyclic at 25 °C and 1 atm with a gas flow of 50 mL min^{-1}. The CO_2 adsorption capacity followed the order of CA-Si-0 > CA-Si-0.5 > CA-Si-1 > CA-Si-1.5 > CA-Si-2 > CA-Si-2.5 > CA-Si-03. Silica-free cellulose aerogel showed the highest CO_2 adsorption capacity (3.68 mmol g^{-1}), and the adsorption capacity reduced as silica content increased, while selectivity increased. Detailed analysis revealed that with increasing silica content, the surface area also increased, but CO_2 adsorption capacity decreased. This indicates a reverse trend where a higher surface area does not necessarily enhance adsorption properties, suggesting that cellulose alone could be particularly effective for CO_2 adsorption applications. Similar trends were observed regarding the effect of pore size on CO_2 adsorption

© 2024 The Author(s). *Energy & Environmental Materials* published by John Wiley & Sons Australia, Ltd on behalf of Zhengzhou University.

25750356, 0, Downloaded from https://onlinelibrary.wiley.com/doi/10.1002/eem2.12832, Wiley Online Library on [10/12/2024]. See the Terms and Conditions (https://onlinelibrary.wiley.com/terms-and-conditions) on Wiley Online Library for rules of use; OA articles are governed by the applicable Creative Commons License

Table 5. Type of support for sorbents design and their properties, information about the amine used, adsorption conditions, and corresponding CO_2 adsorption capacity.

Support used	Textural properties SA ($m^2 g^{-1}$), PV ($cm^3 g^{-1}$), PS (nm)	Amine type	Amine loading (wt.%)	Adsorption capacity (mmol g^{-1})	Adsorption conditions	No. of cycle (capacity drop in total cycles)	References
Silica aerogel-MT400	767, 4.2, 42.7	AP-TMS	1.59[a]	0.67	100% CO_2, 100 mL min^{-1}, Ads.: 25 °C, Des.: 80 °C for 30 min with 100% Argon		[86]
		AEAP-TMS	3.45[a]	1.2			
		DETA-TMS	4.13[a]	1.64			
		TEPA	70	2.50		100 (∼1 wt.%.)	
Aerogel300/95		DETA-TMS	7.4[a]	2.61		100 (∼2wt.%)	
Silica aerogel (SSA)	541, 1.48, 3–20	SASA-1	4.38[a]	1	1% dry CO_2, 300 mL min^{-1}, Ads.: 35 °C	10 (neg.)	[87]
	255, 0.55, 3–15	SASA-3	4.52[a]	1.56	Des.: 90 °C		
	203, 0.48, 3–15	SASA-5	3.86[a]	1.54			
	123, 0.23, 3–10	SASA-7	1.45[a]	0.45			
Silica gel beads	304.7, 0.38, 200–400	0	0	0.21	100% CO_2, 50 mL min^{-1} Ads.: 50 °C	-	[88]
		AP-TMS	12.5	0.67			
		PEI	20	1.16			
Amine hybrid titania/silsesquioxane composite aerogel (AHTSA)	AT-10: 138, 8.48, 3–80	Primary amine (AP-TMS)	8.47[a]	6.66 (10% CO_2)	Ads.: 30 °C, 300 mL min^{-1}, Des.: 90 °C in N_2	15 (neg.)	[96]
				4.19 (1% CO_2)			
				1.64 (0.04% CO_2)			
Zirconia/silica composite aerogel (AHZSA)	54.6, 6.76, 3–80	Primary amine (AP-TMS)	9.60[a]	2.70 (30 °C)	1% CO_2, 300 mL min^{-1}, Des.: 70–120 °C	30 (neg.) Des.: 90 °C	[97]
				2.10 (50 °C)			
				2.00 (70 °C)			
				1.48 (90 °C)			
Hydrophilic Silica aerogel (SA-1)	822, 5, 42	TEPA	80	6.1	100% CO_2, 100 mL min^{-1}, 60 min Ads.: 75 °C Des.: 75 °C in 100% Argon, 100 mL min^{-1}, 20 min	10 (neg)	[103]
				3.5	10% CO_2 Ads.: 75 °C		
Hydrophobic Silica aerogel (SA-O)	673, 3.5, 21	TEPA	80	3.5	100% CO_2, 100 mL min^{-1}, 60 min Ads.: 75 °C		
Silica-cellulose composite aerogel	154.15, 0.81, 22.12	CA-Si-0	0	3.75	100% CO_2, 50 mL min^{-1} Ads.: 25 °C, Des.: 110 °C, dry N_2, 12 hr	–	[106]
	162.65, 0.76, 22.75	CA-Si-0.5	0	3.5			
	282.79, 0.93, 18.56	CA-Si-1	0	2.7			
	333.13, 0.94, 17.16	CA-Si-1.5	0	1.9			
	356.98, 0.86, 15.62	CA-Si-2	0	1.36			
	138.94, 0.69, 22.99	CA-Si-2.5	0	1.36			
	180.73, 0.89, 22.14	CA-Si-3	0	1.02			

© 2024 The Author(s). *Energy & Environmental Materials* published by John Wiley & Sons Australia, Ltd on behalf of Zhengzhou University.

25750356, 0, Downloaded from https://onlinelibrary.wiley.com/doi/10.1002/eem2.12832, Wiley Online Library on [10/12/2024]. See the Terms and Conditions (https://onlinelibrary.wiley.com/terms-and-conditions) on Wiley Online Library for rules of use; OA articles are governed by the applicable Creative Commons License

Table 5. Continued

Support used	Textural properties SA ($m^2 g^{-1}$), PV ($cm^3 g^{-1}$), PS (nm)	Amine type	Amine loading (wt.%)	Adsorption capacity (mmol g^{-1})	Adsorption conditions	No. of cycle (capacity drop in total cycles)	References
Silica gel 200 + deep eutectic solvent	398, 0.78, 6.2	25% ChCl:U:PEI	11.3 atom%	1.15	100% CO_2, 10 mL min^{-1}	8 (~5%)	[108]
		PEI	22	1.09	Ads: 25 °C		

[a]Nitrogen contents (mmol g^{-1}) #in presence of moisture.

capacity, and selectivity. CA-Si-0 and CA-Si-0.5 showed average pore sizes around 31 nm, while other samples exhibited pore sizes in the range of 30–50 nm. As silica content increased, the pore intensity shifted to around 50 nm to super mesopores materials with larger pores and greater heterogeneity. However, as pore size increased, the CO_2 adsorption capacity reduced, indicating that ultra-large pores are not beneficial for adsorption. Nonetheless, selectivity for CO_2 over N_2 increased. Additionally, CO_2 adsorption capacity decreased with increasing temperature, suggesting that the adsorption process is primarily physical adsorption.

5. Deep Eutectic Solvent Functionalized Silica Gel Amine Sorbent

Deep eutectic solvent (DES) has been proposed as a promising green alternative for various applications including CO_2 adsorption. The mixture of urea and choline chloride is used to prepare a non-toxic, and biodegradable DES.[107] Ghazali et al.[108] used SG (SG200) to prepare composite sorbents using a mixture of choline chloride:urea:PEI through a wet-impregnation process. The surface area of SG200 significantly decreased from 398 to 193 $m^2 g^{-1}$ after 22 wt.% PEI loading, but the adsorption capacity improved.[108] The sorption capacity was 51, 48, and 43 mg g^{-1} at 25 °C and 1 bar for 25% ChCl:U:PEI, 22% PEI, and 24% ChCl: PEI, respectively. The effect of temperature was also investigated, showing a decrease in adsorption capacity from 45 mg g^{-1} at 30 °C to 42 mg g^{-1} at 45 °C, with a further decreased at 75 and 85 °C. This is likely due to increasing the mobility of CO_2 which weakens the interaction between CO_2 and NH_2. The presence of ionic liquid may enhance desorption performance of the solid sorbent. The presence of DES in the SG pores might help in thermal heat transfer which may reduce the heat of regeneration. Recyclability studies of composite sorbents using the best sample i.e., 25% ChCl:U:PEI, showed that the composite sorbents remained stable up to eight consecutive cycles.

6. Viewpoints on Solid Amine Sorbent Design and their Applications

SG is available commercially in a wide variety and costs can be in the range of 71–700 \$ kg^{-1}, depending on mesh size and suppliers (**Figure 8a**). However, larger mesh size is not suitable for impregnation or grafting, because of the reduced number of surfaces per unit mass. Therefore, SG with a mesh size of up to 200 and a high surface area (800 $m^2 g^{-1}$) appeared economically viable for large-scale production of SAS. The type of amine needed for SAS also depends on the regeneration conditions. SAS are typically desorbed above 100 °C, with the most effective temperature of 120 °C if no inert gas is used as a sweep gas. Even a reduced pressure could support efficient desorption of SAS at temperatures lower than 120 °C. A higher temperature is preferred if fast desorption is required, although this could lead to amine leaching and degradation.

For desorption temperature analysis, TEPA is taken as a reference, its boiling point (340 °C) is much higher than the desorption temperature required to regenerate SAS (Figure 8b). Despite this high boiling point, various reports stated that TEPA leached out from support easily during the adsorption–desorption cycle; however, extensively studied as a result of academic curiosity.[109] HMW PEI is another amine type that

© 2024 The Author(s). Energy & Environmental Materials published by John Wiley & Sons Australia, Ltd on behalf of Zhengzhou University.

25750356, 0, Downloaded from https://onlinelibrary.wiley.com/doi/10.1002/eem2.12832, Wiley Online Library on [10/12/2024]. See the Terms and Conditions (https://onlinelibrary.wiley.com/terms-and-conditions) on Wiley Online Library for rules of use; OA articles are governed by the applicable Creative Commons License

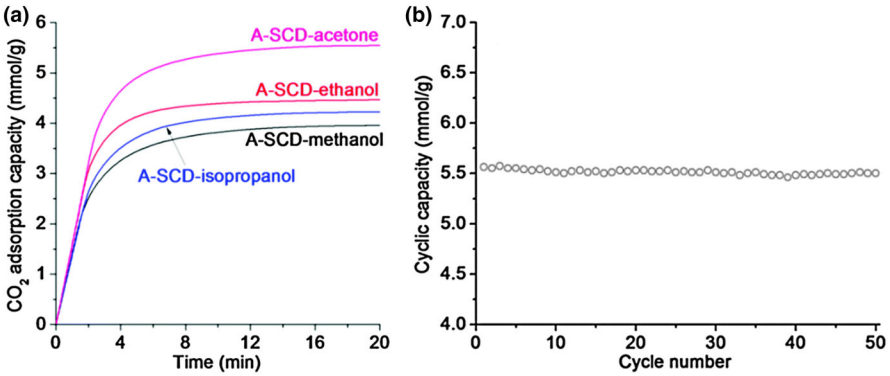

Figure 7. a) Adsorption kinetics at 25 °C, adsorption time 20 min, gas flow 300 mL min^{-1}, 1% moisture. b) cyclic adsorption–desorption at 25 °C, adsorption time 20 min, desorption temperature 90 °C, gas flow 300 mL min^{-1}, 1% moisture. The figure is produced with permission, Copyright, Royal Society of Chemistry.[104]

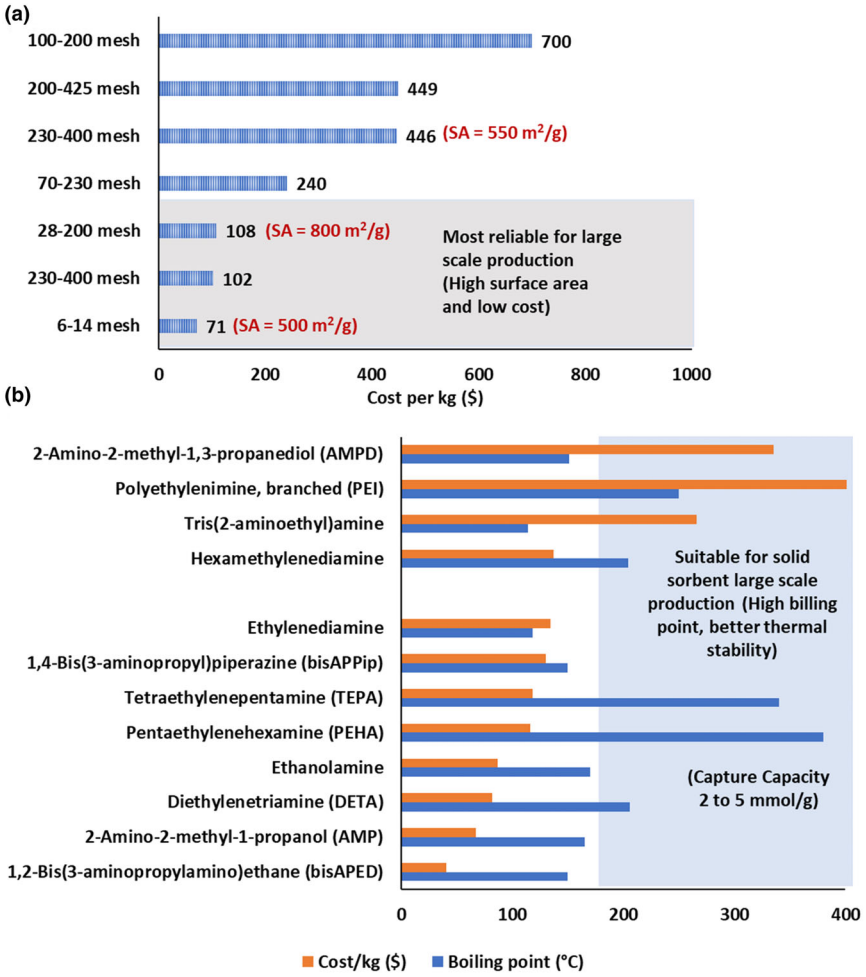

Figure 8. Sorbent cost analysis a) SG cost concerning mesh size and most reliable SG could be explored for large-scale applications. b) Commercially available amine for large-scale solid sorbents production and reliable range.

is more stable than TEPA despite its low boiling point (~280 °C) and is explored for CO_2 capture applications. The HMW of PEI, with a branched structure allows multiple interaction sites with support, helping it to be stabilized against degradation, and leaching during the cyclic adsorption–desorption study.[43] However, amines with shorter chains exhibited high adsorption–desorption rates, due to the combined effects of less diffusion resistance and rapid reaction of primary amines with CO_2.[110]

In other studies, TEPA and PEI polyamines were also modified using epoxide to make them oxidation resistant,[110] enabling them to adsorb CO_2 from various sources including air.[111,112] A 30 wt.% amine loading on any porous material is sufficient to capture CO_2 without compromising diffusion and cost. One kilogram amine can be easily impregnated on 3 kg silica support, which led to the production of around 4 kg in total sorbent. Roughly, the laboratory-scale SAS can cost in the range of $200–1000/kg (depending on the amine and SG type used); however, it can be reduced to below $1/kg at the industrial level.[113]

Pore size and surface area are crucial for designing efficient CO_2 capture sorbents, particularly amine-functionalized materials. High surface area support materials offer more sites for amine groups to be attached and provide a wide surface for uniform distribution, which can increase the number of active site accessibility for CO_2 adsorption. This extensive surface area ensures a higher amine loading, enhancing the overall CO_2 capture capacity. Pore size (in the range of 3–6 nm for SG) also significantly affects the distributions and accessibility of these amine groups. Micropores with a diameter less than 2 nm solely help in the physical adsorption of CO_2; however, completely blocked with amine loading, which restricts the movement and diffusion of CO_2, leading to slower capture rates. Mesopores (which is the case of SG) allow better diffusion and transport of CO_2 molecules. The optimal pore size and structure not only ensure a uniform distribution of amine groups throughout the material but also maximize the overall capture efficiency by leveraging both high surface area and efficient pore accessibility. Thus, tailoring pore size and surface area is vital for

© 2024 The Author(s). *Energy & Environmental Materials* published by John Wiley & Sons Australia, Ltd on behalf of Zhengzhou University.

25750356, 0, Downloaded from https://onlinelibrary.wiley.com/doi/10.1002/eem2.12832, Wiley Online Library on [10/12/2024]. See the Terms and Conditions (https://onlinelibrary.wiley.com/terms-and-conditions) on Wiley Online Library for rules of use; OA articles are governed by the applicable Creative Commons License

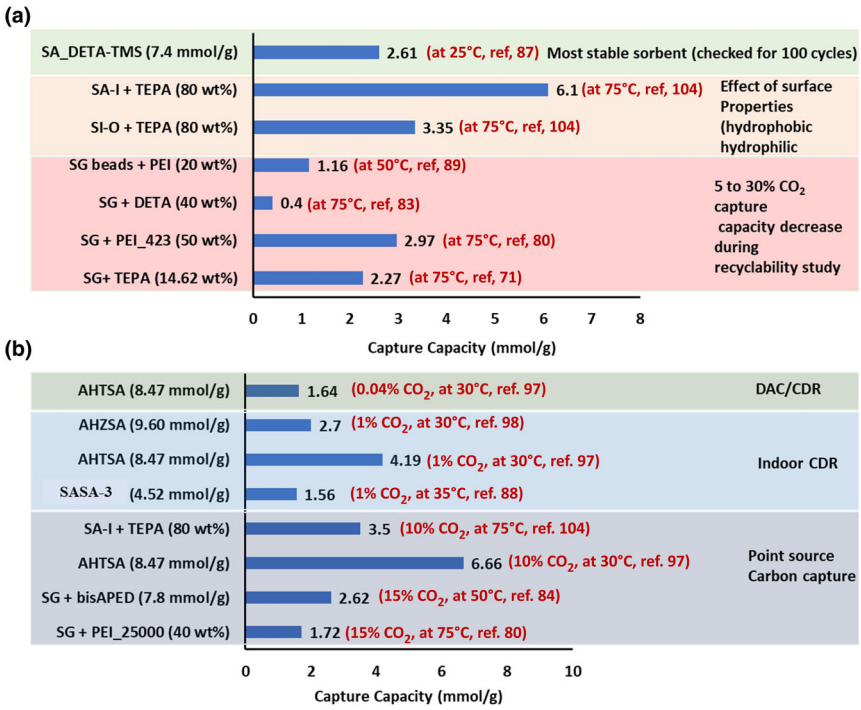

Figure 9. a) CO_2 adsorption studies using 100% CO_2. b) CO_2 adsorption using diluted CO_2 gas. In a and b, the sample name (nitrogen contents are given in wt.% or mmol g^{-1}).

enhancing the performance of amine-functionalized materials in CO_2 capture applications, contributing significantly to efforts in reducing carbon emissions and mitigating climate change. Despite pore size, the pore length of support materials also significantly affects the adsorption performance, and materials with short channels showed the fastest adsorption and highest capacity. Short pore length of support material improved amine accessibility inside the pores and diminished diffusion resistance.[114]

G-based SAS development has not been explored and investigated for large-scale applications and has mostly been studied for fundamental understanding. The use of a gas mixture of more than 15% CO_2 has limited relevance to industrial applications, with few studies conducted using 100% CO_2 significantly inflating adsorption values up to 2–3 times. Therefore, in such conditions, sorbents do not represent their actual adsorption capacity for the actual applied CO_2 capture applications of industrial relevance. For industrial-grade SAS, CO_2 concentration in the range of 1–15% CO_2 or compressed air should ideally be used. A comparison between the adsorption capacity when CO_2 is 100% or 1–15% can be easily done based on data given in Table 3. For example, Zhang et al.[79] indicated that for PEI(423)/SG (mesh size 33–75), CO_2 adsorption capacity increased from 60.6 to 131.1 mg g^{-1} when CO_2 concentration changed from 15% to 100% CO_2. A very interesting relationship between SG mesh size and PEI molecular weight was observed, noting that CO_2 adsorption capacity decreased with the SG mesh size and PEI molecular weight increased.

For the comparison of CO_2 adsorption capacity using pure CO_2 instead of diluted CO_2, covalently functionalized SA outperformed most of the sorbents in terms of recyclability (**Figure 9**a). Triamine (DETA-TMS) functionalized SA showed the average adsorption capacity of 2.61 mmol g^{-1} and only 2% change in 100 cycles, making them suitable for industrial applications.[86] TEPA functionalized SA-I also exhibited a very impressive CO_2 adsorption capacity of 6.1 mmol g^{-1} at 75 °C;[103] however, TEPA is known for fast degradation and leaching during the cyclic study of CO_2 capture. Since SA-I outperformed SA-O, moisture or water have a positive role in CO_2 adsorption (Figure 8a).

Diluted CO_2 gas (400 ppm to 15%) can provide more reliable data to develop and upscale industrial facilities for DAC, and the use of pure gas is far from the reality (Figure 9b). AHTSA exhibited a very high adsorption capacity of 6.66 mmol g^{-1} for 10% CO_2 which is relevant for industrial applications.[96] Amine-based aerogel sorbents were also explored for 1% CO_2, which are suitable for indoor CO_2 adsorption applications at large commercial spaces, such as malls, offices, etc. AHTSA also showed an impressive CO_2 adsorption capacity of 4.19 mmol g^{-1} for 1% CO_2 at 30 °C (Figure 9b).[96] Similarly, the same material was also used for 400 ppm CO_2 adsorption, which is the most reliable condition for DAC. Hence, for an industrial facility for DAC, PSCC, or indoor CO_2 adsorption, we must develop highly stable, large-capacity, easy-to-upscale industrial-grade sorbent pellets instead of powder. These findings are inspiring and motivating to develop amine-based solid sorbents for large-scale CO_2 adsorption.

7. Conclusion

Based on the reports, solid sorbents for CO_2 adsorption can be categorized into four different classes:

Class-1: Physisorption of amines on porous materials. Class-2: Amines are covalently attached to the surface of support materials through the amino silane chemistry. Class-3: Materials developed by the polymerization of amine monomers within the pore volume, in-situ polymerization of silica precursor and amino silane. Class-4: A mixture of different amines adsorbed on solid support.

Class-1 sorbent contains substantial amounts of amines on porous support and has a large CO_2 adsorption capacity. However, Class-1 faces many challenges such as low thermal stability, oxidative degradation, and leaching of physisorbed amine during recycling. Class-2 sorbents have better thermal stability compared to Class-1; however, Class-2 is limited by amine loading due to the availability of surface silanol (-Si-OH) sites for covalent functionalization. Class-3 sorbents are less explored, and their low surface area, pore volume, and high production cost limit large-scale production. Class-4 is the least explored in the series and progress is still being made, as blending two or more varieties of amines could improve the performance and slow the degradation of amines during recycling.

Commercial SG is mostly produced by polymerization of a sodium silicate precursor via mixing with HCl or H_2SO_4. SG with a wide range of desired textural properties such as wide pore size distribution, high

© 2024 The Author(s). *Energy & Environmental Materials* published by John Wiley & Sons Australia, Ltd on behalf of Zhengzhou University.

25750356, 0, Downloaded from https://onlinelibrary.wiley.com/doi/10.1002/eem2.12832, Wiley Online Library on [10/12/2024]. See the Terms and Conditions (https://onlinelibrary.wiley.com/terms-and-conditions) on Wiley Online Library for rules of use; OA articles are governed by the applicable Creative Commons License

surface area, and large pore volume can be produced by controlling the polymerization conditions such as silicate concentration, temperature, time, and pH. Compared to mesoporous silica such as SBA-15, MCM-41, KCC-1, and cellular silica, SG is commercially available in large quantities and at a substantially lower cost (Table 1).

Mesoporous silica is mostly produced in the fine powder form which cannot be utilized directly and needs to be pelletized before it can be used for fixed bed or moving bed adsorption applications. However, larger mesh-size SG particles can be explored for amine grafting and adsorption applications without shaping into pellets or beads. Easy to synthesize, low carbon footprints, no dangerous by-products during processing, and easy to scale up at the industrial level are the key criteria for industrial-grade sorbent design and large-scale CO_2 capture facility development. It is crucial to develop low-carbon footprint sorbents. High CO_2 adsorption capacity with large carbon footprint sorbents would not make a meaningful impact. Based on the author's understanding and experience, the following points should be explored to develop sustainable and scalable SAS for large-scale CO_2 capture applications:

1 The cost of sorbent design: Low-cost industrial-grade sorbents are highly demanded. Using commercially available SG as a support material for large-scale CO_2 capture could be beneficial. The cost and carbon footprint of the complete process are crucial. The development of an industrial process is tedious, time-consuming, and expensive. Using commercially available support materials for grafting amine (covalent or physisorbed) could reduce costs. SG, as a cheap, biodegradable, and easy-to-modify surface may lead to the development of large-scale sorbents for industrial applications.In this regard, the following points should be considered: Industrial Grade Sorbents: Industries mostly prefer sorbent pellets not powder, hence, sorbent preparation and performance check at a laboratory scale (minimum 100 to 1000 gm) should be performed after shaping powder into pellets, monoliths, beads, etc. The carbon footprint of sorbent production including CO_2 emission by support synthesis, amines production, and CO_2 emission after end life, must be calculated and counted.[115]
2 Thermal and Chemical Stability: Varieties of amines were explored for CO_2 capture at laboratory scales. Some of the amine-based monolithic sorbents are also designed to capture CO_2 from the air. Most amines are prone to oxidative degradation with cyclic adsorption–desorption, and the formation of permanent thermally stable molecular species like urea can degrade adsorption capacity. This is a major limitation, and research should be focused on increasing the chemical and thermal stability of amine-based solid sorbents to decrease CO_2 capture costs further.
3 Desorption performance: SAS need to be heated in the range of 100–120 °C, using N_2 as a sweep gas (if TGA is used to investigate CO_2 adsorption capacity). When inert gas is used to sweep CO_2 from sorbents, it decreases the gas purity. Cyclic adsorption–desorption test should be performed without the use of sweep gas; however, it is a standard practice when sorbents are analyzed using TGA. Hence, to validate the sorbents for large-scale CO_2 capture applications, breakthrough curves, and cyclic adsorption–desorption should be performed at least at the kg scale, using a fixed bed reactor without sweep gas.
4 Sample analysis in real conditions: On the laboratory scale, most of the sorbents are analyzed using either 100% CO_2 or diluted CO_2 in N_2 (mixed at the desired concentrations). If sorbents are developed for PSCC, then sorbents should be tested for NO_x and SO_x impurities as well. However, NO_x and SO_x abatement with sorbents are already in practice at the industrial level. For DAC, sorbent must be screened for compressed air instead of CO_2 (400 ppm) in N_2, and the effect of moisture should be considered.
5 (Process design for) Pellets recycling: At an industrial level, most sorbents are utilized in the form of pellets or monoliths. These sorbents are either composed of silica, alumina, or zirconia, and most of them are produced at large scale. For large-scale CO_2 capture, millions of tons of these pellets are needed. If they are produced for single use and disposal, this will result in solid industrial waste. Therefore, these pellets need to be re-utilized, recycled and reshaped again.[116] However, investigations and demonstrations of such processes are necessary but have not yet been performed.

Acknowledgement

B.S. and T.R. are grateful for financial support from Business Finland 8205/31/2022. Z.E. would like to thank the Magnus Ehrnrooth Foundation for financial support.

Conflict of Interest

The authors declare no competing financial interest.

Author Contributions

BS was involved in conceptualization, analysis, visualization, writing original draft, editing and management. ZEG, RS, VS, and TR were involved in editing and supporting final draft preparation. ZEG was involved in graphical abstract.

Keywords

direct air capture, point source CO_2 capture, silica gel, solid amine sorbent

Received: March 28, 2024
Revised: June 24, 2024
Published online: August 14, 2024

[1] M. Honegger, *Nat. Commun.* **2023**, *14*, 534.
[2] Y. Jiang, P. M. Mathias, R. F. Zheng, C. J. Freeman, D. Barpaga, D. Malhotra, P. K. Koech, A. Zwoster, D. J. Heldebrant, *J. Clean. Prod.* **2023**, *388*, 135696.
[3] J. Gibbins, H. Chalmers, M. Lucquiaud, J. Li, N. McGlashan, X. Liang, J. Davison, *Energy Procedia* **2011**, *4*, 1835.
[4] A. Richard, C. D. J. Betts, J. R. Knight, J. O. Pope, C. Sandford, Mauna Loa carbon dioxide forecast for 2024: Atmospheric CO_2 rise predicted to exceed IPCC 1.5°C scenarios. https://www.metoffice.gov.uk/research/climate/seasonal-to-decadal/long-range/forecasts/co2-forecast-for-2024

© 2024 The Author(s). *Energy & Environmental Materials* published by John Wiley & Sons Australia, Ltd on behalf of Zhengzhou University.

25750356, 0, Downloaded from https://onlinelibrary.wiley.com/doi/10.1002/eem2.12832, Wiley Online Library on [10/12/2024]. See the Terms and Conditions (https://onlinelibrary.wiley.com/terms-and-conditions) on Wiley Online Library for rules of use; OA articles are governed by the applicable Creative Commons License

[5] M. W. Jones, G. P. Peters, T. Gasser, R. M. Andrew, C. Schwingshackl, J. Gütschow, R. A. Houghton, P. Friedlingstein, J. Pongratz, C. Le Quéré, *Scientific Data* **2023**, *10*, 155.
[6] X. Lan, P. Tans, K. W. Thoning, Trends in globally-averaged CO_2 determined from NOAA 16 Global Monitoring Laboratory measurements. 10.15138/9N0H-ZH07.
[7] H. C. Lau, S. Ramakrishna, K. Zhang, A. V. Radhamani, *Energy Fuel* **2021**, *35*, 7364.
[8] B. Singh, M. Kemell, and T. Repo, *Mater. Adv.* **2024**, https://doi.org/10.1039/D4MA00703D
[9] M. R. Ketabchi, S. Babamohammadi, W. G. Davies, M. Gorbounov, S. Masoudi Soltani, *Carbon Capture Sci. Technol.* **2023**, *6*, 100087.
[10] R. Chang, X. Wu, O. Cheung, W. Liu, *J. Mat. Chem. A* **2022**, *10*, 1682.
[11] J. Wang, L. Huang, R. Yang, Z. Zhang, J. Wu, Y. Gao, Q. Wang, D. O'Hare, Z. Zhong, *Energy Environ. Sci.* **2014**, *7*, 3478.
[12] A. Sodiq, Y. Abdullatif, B. Aissa, A. Ostovar, N. Nassar, M. El-Naas, A. Amhamed, *Environ. Technol. Innov.* **2023**, *29*, 102991.
[13] Y. Abdullatif, A. Sodiq, N. Mir, Y. Bicer, T. Al-Ansari, M. H. El-Naas, A. I. Amhamed, *RSC Adv.* **2023**, *13*, 5687.
[14] F. Raganati, F. Miccio, P. Ammendola, *Energy Fuel* **2021**, *35*, 12845.
[15] A. Samanta, A. Zhao, G. K. H. Shimizu, P. Sarkar, R. Gupta, *Ind. Eng. Chem. Res.* **2012**, *51*, 1438.
[16] F. O. Ochedi, J. Yu, H. Yu, Y. Liu, A. Hussain, *Environ. Chem. Lett.* **2021**, *19*, 77.
[17] W. Yu, T. Wang, A.-H. A. Park, M. Fang, *Nanoscale* **2019**, *11*, 17137.
[18] N. Hussain Solangi, F. Hussin, A. Anjum, N. Sabzoi, S. Ali Mazari, N. M. Mubarak, M. Kheireddine Aroua, M. T. H. Siddiqui, S. Saeed Qureshi, *J. Mol. Liq.* **2023**, *374*, 121266.
[19] B. Aghel, S. Janati, S. Wongwises, M. S. Shadloo, *Int. J. Greenhouse Gas Control* **2022**, *119*, 103715.
[20] S. Sun, H. Sun, P. T. Williams, C. Wu, *Sustain. Energy Fuels* **2021**, *5*, 4546.
[21] E. S. Sanz-Pérez, C. R. Murdock, S. A. Didas, C. W. Jones, *Chem. Rev.* **2016**, *116*, 11840.
[22] E. E. Ünveren, B. Ö. Monkul, Ş. Sarıoğlan, N. Karademir, E. Alper, *Petroleum* **2017**, *3*, 37.
[23] M. T. Dunstan, F. Donat, A. H. Bork, C. P. Grey, C. R. Müller, *Chem. Rev.* **2021**, *121*, 12681.
[24] L. Shi, L. S. Lai, W. H. Tay, S. P. Yeap, Y. F. Yeong, *ChemBioEng Rev.* **2022**, *9*, 556.
[25] N. Norahim, P. Yaisanga, K. Faungnawakij, T. Charinpanitkul, C. Klaysom, *Chem. Eng. Technol.* **2018**, *41*, 211.
[26] Y. Han, W. S. W. Ho, *J. Membr. Sci.* **2021**, *628*, 119244.
[27] G. Chen, T. Wang, G. Zhang, G. Liu, W. Jin, *Adv. Membr.* **2022**, *2*, 100025.
[28] S. Fujikawa, R. Selyanchyn, T. Kunitake, *Polym. J.* **2021**, *53*, 111.
[29] R. Ben-Mansour, M. A. Habib, O. E. Bamidele, M. Basha, N. A. A. Qasem, A. Peedikakkal, T. Laoui, M. Ali, *Appl. Energy* **2016**, *161*, 225.
[30] A. H. Berger, A. S. Bhown, *Energy Procedia* **2011**, *4*, 562.
[31] R.-S. Liu, X.-D. Shi, C.-T. Wang, Y.-Z. Gao, S. Xu, G.-P. Hao, S. Chen, A.-H. Lu, *ChemSusChem* **2021**, *14*, 1428.
[32] M. M. Yassin, J. A. Anderson, G. A. Dimitrakis, C. F. Martín, *Sep. Purif. Technol.* **2021**, *276*, 119326.
[33] Z. Cui, Q. Du, J. Gao, R. Bie, *Appl. Therm. Eng.* **2023**, *230*, 120834.
[34] X. Chen, J. Wang, T. Ren, Z. Li, T. Du, X. Lu, L. Liu, Y. Wang, D. Xu, C. Chang, W. Tan, G. K. Li, *Sep. Purif. Technol.* **2023**, *308*, 122837.
[35] F. Su, C. Lu, *Energy Environ. Sci.* **2012**, *5*, 9021.
[36] A. Ntiamoah, J. Ling, P. Xiao, P. A. Webley, Y. Zhai, *Ind. Eng. Chem. Res.* **2016**, *55*, 703.
[37] M. J. Bos, V. Kroeze, S. Sutanto, D. W. F. Brilman, *Ind. Eng. Chem. Res.* **2018**, *57*, 11141.
[38] G. Ji, H. Yang, M. Z. Memon, Y. Gao, B. Qu, W. Fu, G. Olguin, M. Zhao, A. Li, *Appl. Energy* **2020**, *267*, 114874.
[39] S. Wang, Y. Li, Z. Li, *Ind. Eng. Chem. Res.* **2020**, *59*, 6855.
[40] A. Abdollahi-Govar, A. D. Ebner, J. A. Ritter, *Energy Fuel* **2015**, *29*, 4492.
[41] M. J. Al-Marri, Y. O. Kuti, M. Khraisheh, A. Kumar, M. M. Khader, *Chem. Eng. Technol.* **2017**, *40*, 1802.
[42] N. Masoud, G. Bordanaba-Florit, T. van Haasterecht, J. H. Bitter, *Ind. Eng. Chem. Res.* **2021**, *60*, 13749.
[43] K. Maresz, A. Ciemięga, J. J. Malinowski, J. Mrowiec-Białoń, *Chem. Eng. J.* **2020**, *383*, 123175.
[44] S. J. Vevelstad, V. Buvik, H. K. Knuutila, A. Grimstvedt, E. F. da Silva, *Ind. Eng. Chem. Res.* **2022**, *61*, 15737.
[45] Y. Ding, L. Ma, F. Zeng, X. Zhao, H. Wang, X. Zhu, Q. Liao, *Energy* **2023**, *263*, 125723.
[46] F. Rezaei, C. W. Jones, *Ind. Eng. Chem. Res.* **2013**, *52*, 12192.
[47] J. Yu, S. S. C. Chuang, *Ind. Eng. Chem. Res.* **2017**, *56*, 6337.
[48] J. Yu, Y. Zhai, S. S. C. Chuang, *Ind. Eng. Chem. Res.* **2018**, *57*, 4052.
[49] R. Veneman, N. Frigka, W. Zhao, Z. Li, S. Kersten, W. Brilman, *Int. J Greenhouse Gas Control* **2015**, *41*, 268.
[50] J. Young, E. García-Díez, S. Garcia, M. van der Spek, *Environ. Sci.* **2021**, *14*, 5377.
[51] C. Drechsler, D. W. Agar, *Energy* **2020**, *192*, 116587.
[52] K. Fu, M. Zheng, H. Wang, D. Fu, *Energy* **2022**, *244*, 122656.
[53] J. M. Kolle, M. Fayaz, A. Sayari, *Chem. Rev.* **2021**, *121*, 7280.
[54] R. Belgamwar, A. Maity, T. Das, S. Chakraborty, C. P. Vinod, V. Polshettiwar, *Chem. Sci.* **2021**, *12*, 4825.
[55] W. Zhao, Z. Zhang, Z. Li, N. Cai, *Ind. Eng. Chem. Res.* **2013**, *52*, 2084.
[56] R. A. Khatri, S. S. C. Chuang, Y. Soong, M. Gray, *Energy Fuel* **2006**, *20*, 1514.
[57] S. G. Subraveti, S. Roussanaly, R. Anantharaman, L. Riboldi, A. Rajendran, *Appl. Energy* **2022**, *306*, 117955.
[58] J. F. Wiegner, A. Grimm, L. Weimann, M. Gazzani, *Ind. Eng. Chem. Res.* **2022**, *61*, 12649.
[59] B. Singh, J. Na, M. Konarova, T. Wakihara, Y. Yamauchi, C. Salomon, M. B. Gawande, *Bull. Chem. Soc. Jpn.* **2020**, *93*, 1459.
[60] B. Singh, V. Polshettiwar, *J. Mater. Chem. A* **2016**, *4*, 7005.
[61] N. Bayal, B. Singh, R. Singh, V. Polshettiwar, *Sci. Rep.* **2016**, *6*, 24888.
[62] B. Singh, V. Polshettiwar, *Nanoscale* **2019**, *11*, 5365.
[63] B. Singh, A. Maity, V. Polshettiwar, *ChemistrySelect* **2018**, *3*, 10684.
[64] X. Shen, H. Du, R. H. Mullins, R. R. Kommalapati, *Energy* **2017**, *5*, 822.
[65] Y. Fan, X. Jia, *Energy Fuel* **2022**, *36*, 1252.
[66] J. D. Lunn, D. F. Shantz, *Chem. Mater.* **2009**, *21*, 3638.
[67] S. A. Didas, S. Choi, W. Chaikittisilp, C. W. Jones, *Acc. Chem. Res.* **2015**, *48*, 2680.
[68] D. J. Fauth, M. L. Gray, H. W. Pennline, H. M. Krutka, S. Sjostrom, A. M. Ault, *Energy Fuel* **2012**, *26*, 2483.
[69] D. S. Dao, H. Yamada, K. Yogo, *Ind. Eng. Chem. Res.* **2013**, *52*, 13810.
[70] C. Chen, S. Bhattacharjee, *Greenhouse Gases Sci. Technol.* **2017**, *7*, 1116.
[71] Y. G. Ko, S. S. Shin, U. S. Choi, *J. Colloid Interface Sci.* **2011**, *361*, 594.
[72] Y. Teng, Z. Liu, G. Xu, K. Zhang, *Energies* **2017**, *10*, 115.
[73] C.-H. Yu, C.-H. Huang, C.-S. Tan, *Aerosol Air Qual. Res.* **2012**, *12*, 745.
[74] K. Wang, H. Shang, L. Li, X. Yan, Z. Yan, C. Liu, Q. Zha, *J. Nat. Gas Chem.* **2012**, *21*, 319.
[75] D. Wang, C. Sentorun-Shalaby, X. Ma, C. Song, *Energy Fuel* **2011**, *25*, 456.
[76] X. Yan, Y. Zhang, K. Qiao, X. Li, Z. Zhang, Z. Yan, S. Komarneni, *J. Hazard. Mater.* **2011**, *192*, 1505.
[77] J. Hack, N. Maeda, D. M. Meier, *ACS Omega* **2022**, *7*, 39520.
[78] Y. Shi, Q. Liu, Y. He, in *Handbook of Climate Change Mitigation and Adaptation* (Eds: W.-Y. Chen, T. Suzuki, M. Lackner), Springer New York, New York, NY **2014**, p. 1.
[79] Z. Zhang, X. Ma, D. Wang, C. Song, Y. Wang, *AIChE J* **2012**, *58*, 2495.
[80] B. Singh, K. R. Mote, C. S. Gopinath, P. K. Madhu, V. Polshettiwar, *Angew. Chem. Int. Ed.* **2015**, *54*, 5985.
[81] B. Singh, V. Polshettiwar, *Pure Appl. Chem.* **2023**, *95*, 451.

© 2024 The Author(s). *Energy & Environmental Materials* published by John Wiley & Sons Australia, Ltd on behalf of Zhengzhou University.

25750356, 0, Downloaded from https://onlinelibrary.wiley.com/doi/10.1002/eem2.12832, Wiley Online Library on [10/12/2024]. See the Terms and Conditions (https://onlinelibrary.wiley.com/terms-and-conditions) on Wiley Online Library for rules of use; OA articles are governed by the applicable Creative Commons License

[82] C. F. Martín, M. B. Sweatman, S. Brandani, X. Fan, *Appl. Energy* **2016**, *183*, 1705.
[83] G. D. Pirngruber, S. Cassiano-Gaspar, S. Louret, A. Chaumonnot, B. Delfort, *Energy Procedia* **2009**, *1*, 1335.
[84] J.-T. Anyanwu, Y. Wang, R. T. Yang, *Ind. Eng. Chem. Res.* **2020**, *59*, 7072.
[85] H. Jung, C. H. Lee, S. Jeon, D. H. Jo, J. Huh, S. H. Kim, *Adsorption* **2016**, *22*, 1137.
[86] N. N. Linneen, R. Pfeffer, Y. S. Lin, *Chem. Eng. J.* **2014**, *254*, 190.
[87] X. Jiang, Y. Kong, Z. Zhao, X. Shen, *RSC Adv.* **2020**, *10*, 25911.
[88] N. Minju, P. Abhilash, B. N. Nair, A. P. Mohamed, S. Ananthakumar, *Chem. Eng. J.* **2015**, *269*, 335.
[89] N. N. Linneen, R. Pfeffer, Y. S. Lin, *Ind. Eng. Chem. Res.* **2013**, *52*, 14671.
[90] Z. Wang, Z. Dai, J. Wu, N. Zhao, J. Xu, *Adv. Mater.* **2013**, *25*, 4494.
[91] K. Wörmeyer, I. Smirnova, *Microporous Mesoporous Mater.* **2014**, *184*, 61.
[92] K. Wörmeyer, M. Alnaief, I. Smirnova, *Adsorption* **2012**, *18*, 163.
[93] K. Wörmeyer, I. Smirnova, *Chem. Eng. J.* **2013**, *225*, 350.
[94] Z. Zhang, S. Zhao, Z. Fei, K. Li, G. Chen, J. Chen, P. Zhang, Z. Yang, *ACS Appl. Nano Mater.* **2023**, *6*, 1927.
[95] Y. Kong, X. Shen, M. Fan, M. Yang, S. Cui, *Chem. Eng. J.* **2016**, *283*, 1059.
[96] Y. Kong, G. Jiang, Y. Wu, S. Cui, X. Shen, *Chem. Eng. J.* **2016**, *306*, 362.
[97] Y. Kong, X. Shen, S. Cui, *Microporous Mesoporous Mater.* **2016**, *236*, 269.
[98] Y. Kong, X. Shen, S. Cui, M. Fan, *Green Chem.* **2015**, *17*, 3436.
[99] Y. Kong, X. Shen, S. Cui, M. Fan, *Appl. Energy* **2015**, *147*, 308.
[100] A. A. Alhwaige, T. Agag, H. Ishida, S. Qutubuddin, *RSC Adv.* **2013**, *3*, 16011.
[101] A. A. Alhwaige, H. Ishida, S. Qutubuddin, *ACS Sustain. Chem. Eng.* **2016**, *4*, 1286.
[102] S. Choi, M. L. Gray, C. W. Jones, *ChemSusChem* **2011**, *4*, 628.
[103] N. Linneen, R. Pfeffer, Y. S. Lin, *Microporous Mesoporous Mater.* **2013**, *176*, 123.
[104] Y. Kong, G. Jiang, M. Fan, X. Shen, S. Cui, A. G. Russell, *Chem. Commun.* **2014**, *50*, 12158.
[105] Y. Kong, G. Jiang, M. Fan, X. Shen, S. Cui, *RSC Adv.* **2014**, *4*, 43448.
[106] Y. Miao, M. Pudukudy, Y. Zhi, Y. Miao, S. Shan, Q. Jia, Y. Ni, *Carbohydr. Polym.* **2020**, *236*, 116079.
[107] M. Bisht, B. Bhawna, B. Singh, S. Pandey, *J. Mol. Liq.* **2023**, *384*, 122203.
[108] Z. Ghazali, N. Suhaili, M. N. A. Tahari, M. A. Yarmo, N. H. Hassan, R. Othaman, *J. Mater. Res. Technol.* **2020**, *9*, 3249.
[109] G. Zhang, P. Zhao, Y. Xu, Z. Yang, H. Cheng, Y. Zhang, *ACS Appl. Mater. Interfaces* **2018**, *10*, 34340.
[110] Z. Liu, Y. Teng, K. Zhang, H. Chen, Y. Yang, *J. Energy Chem.* **2015**, *24*, 322.
[111] A. Goeppert, H. Zhang, R. Sen, H. Dang, G. K. S. Prakash, *ChemSusChem* **2019**, *12*, 1712.
[112] W. Choi, K. Min, C. Kim, Y. S. Ko, J. W. Jeon, H. Seo, Y.-K. Park, M. Choi, *Nat. Commun.* **2016**, *7*, 12640.
[113] H. E. Holmes, R. P. Lively, M. J. Realff, *JACS Au* **2021**, *1*, 795.
[114] A. Heydari-Gorji, Y. Yang, A. Sayari, *Energy Fuel* **2011**, *25*, 4206.
[115] G. Leonzio, O. Mwabonje, P. S. Fennell, N. Shah, *Sustain. Prod. Consum.* **2022**, *32*, 101.
[116] B. Singh, M. Kemell, J. Yliniemi, T. Repo, *Nanoscale* **2024**. DOI: 10.1039/D4NR02495H.

© 2024 The Author(s). *Energy & Environmental Materials* published by John Wiley & Sons Australia, Ltd on behalf of Zhengzhou University.

25750356, 0, Downloaded from https://onlinelibrary.wiley.com/doi/10.1002/eem2.12832, Wiley Online Library on [10/12/2024]. See the Terms and Conditions (https://onlinelibrary.wiley.com/terms-and-conditions) on Wiley Online Library for rules of use; OA articles are governed by the applicable Creative Commons License